A THESIS SUBMITTED TO
THE GRADUATE SCHOOL OF NATURAL AND APPLIED SCIENCES
OF ÇANKIRI KARATEKİN UNIVERSITY

RESEARCH ON EXPERIMENTAL PERFORMANCE IN SOLAR WATER HEATING SYSTEMS

IN PARTIAL FULFILLMENT OF THE REQUIREMENTS
FOR
THE DEGREE OF MASTER OF SCIENCE
IN
PHYSICS

BY

Wisam Mohammed Fayyadh FAYYADH

ÇANKIRI

2023

RESEARCH ON EXPERIMENTAL PERFORMANCE IN SOLAR WATER HEATING SYSTEMS

By Wisam Mohammed Fayyadh FAYYADH

February 2023

We certify that we have read this thesis and that in our opinion it is fully adequate, in scope and in quality, as a thesis for the degree of Master of Science

Advisor : Prof. Dr. Halit ALTUNTAŞ
Co-Advisor : Prof. Dr. Yaseen H. MAHMOOD

Examining Committee Members:

Chairman : Prof. Dr. Name SURNAME
Chemical Engineering
Çankırı Karatekin University

Member : Assoc. Prof. Dr. Name SURNAME
Chemical Engineering
Çankırı Karatekin University

Member : Asst. Prof. Dr. Name SURNAME
Chemical Engineering
Çankırı Karatekin University

Approved for the Graduate School of Natural and Applied Sciences

Prof. Dr. İbrahim ÇİFTÇİ
Director of Graduate School

I hereby declare that all information in this document has been obtained and presented in accordance with academic rules and ethical conduct. I also declare that, as required by these rules and conduct, I have fully cited and referenced all material and results that are not original to this work.

Wisam Mohammed Fayyadh FAYYADH

ABSTRACT

RESEARCH ON EXPERIMENTAL PERFORMANCE IN SOLAR WATER HEATING SYSTEMS

Wisam Mohammed Fayyadh FAYYADH
Master of Science in Physics
Advisor: Prof. Dr. Halit ALTUNTAŞ
Co-Advisor: Prof. Dr. Yaseen H. MAHMOOD
February 2023

In this study, a solar dish collector is designed and manufactured. Moreover, its engineering and applied properties, the effect of the change in the mass flow rate 0.0055 kg/s, 0.009 kg/s, 0.022 kg/s, and 0.028 kg/s on the water temperature entering and exiting the receiver, and the efficiency of the collector are all studied. This study aims to heat the working fluid (water) with several variables. The experiments are carried out in Iraq Erbil – Kasnazan at a longitude of 44.12° and latitude of 36.21°. The collector is manufactured from locally available materials, the same dish used in television communications, with a diameter of 1.4 m and a depth of 0.14 m. It is covered with glass as a reflective material cut into square pieces, the dimensions of which are 2×2 cm. It consists of a cylindrical receiver, in which the receiver consists of two pipes made of stainless steel with a thickness of 0.007 m. The first pipe's inner and outer diameters are 0.145 m and 0.152 m, respectively, with a height of 0.23 m. As for the second pipe, the inner and outer diameters are 0.095 m and 0.102 m, respectively. The first is connected to the second by a metal disk of the same thickness attached to the cylinder from the bottom and contains two holes for passing the copper pipe, with a length inside the receiver reaching 12.5 m. The system also consists of a water tank, a metal base to install the solar collector, and an electrical circuit (to track the sun). After installing all the parts in place, the system is operated, and experiments are conducted for the month of May. The results obtained above show that the highest process efficiency obtained in May is on the 16th of May at a mass flow rate of 0.028 kg/s, reaching about 0.82 to 0.90, while the lowest efficiency is on the 6th of May at a mass flow rate of 0.0055 kg/s reaching 0.57 to 0.89. The useful energy absorbed by the water per unit of time as it passes into the receiver is 1281.26 W. This value represents the highest useful energy obtained in the month of April at a flow rate of 0.028 kg/s. The highest temperature of the water exiting the receiver is 413 K on the 6th of May, at a mass flow rate of 0.0055 kg/s. The lowest useful energy absorbed by the water on the 6th of May when passing into the receiver is 1164.50 W at a mass flow rate of 0.0055 kg/s.

2023, 88 pages

Keywords: Solar energy, Solar heating, Thermal efficiency, Heat

ÖZET

GÜNEŞ ENERJILI SU ISITMA SİSTEMLERİNDE DENEYSEL PERFORMANSA BAĞLI ARAŞTIRMA

Wisam Mohammed Fayyadh FAYYADH

Tez Danışmanı: Prof. Dr. HALİT ALTUNTAŞ

Eş Danışman: Prof. Dr. Yaseen H. MAHMOOD

Şubat 2023

Bu çalışmada bir parabolik çanak kollektörü tasarlanmış ve üretilmiştir. Ayrıca mühendislik ve uygulama özellikleri, kütlesel debideki 0,0055 kg/s, 0,009 kg/s, 0,022 kg/s, 0,028 kg/s değişimin alıcıya giren ve alıcıdan çıkan su sıcaklığına ve kollektör verimine etkisi incelenmiştir. Bu araştırmanın amacı, çalışmadaki sıvıyı (su) birkaç değişkenle ısıtmaktır. Deneyler, Iraq Erbil-kasnazan 44,12° boylam ve 36,21° enlemi koordinatlarında gerçekleştirilmiştir. Toplayıcı, yerel olarak bulunabilen malzemelerden imal edilmiştir. Televizyon iletişiminde kullanılan 1,4 m çaplı ve 0,14 m derinliğindeki aynı çanak kullanılmıştır. Yansıtıcı malzeme olarak boyutları 2×2 cm olan kare parçalar halinde kesilmiş cam ile kaplanmıştır. Alıcı 0.007 m kalınlığında paslanmaz çelikten yapılmış iki borudan oluşmakta olup silindirik bir yapıdadır. Birinci borunun iç ve dış boyutları sırasıyla 0,145 m ile 0,152 m çapında ve 0,23 m yüksekliğindedir. İkinci borunun iç ve dış çapları sırasıyla 0,095m ile 0,098m'dir. Birinci boru, alttan silindire tutturulmuş aynı kalınlıkta metal bir diskle ikinci boruya bağlanmaktadır. Alıcının içinde 12,5 m uzunlukta bakır borunun geçirilebilmesi için iki delik, bir su deposu, güneş merkezini kurmak için metal bir taban ve bir elektrik devresi (güneşi izleyen) yer almaktadır. Tüm parçaların kurulumunu yaptıktan sonra sistem çalıştırıldıktan sonra mayıs ayının işlem ölçümleri yapıldı. Yukarıda elde edilen sonuçlar, mayıs ayında elde edilen en yüksek verimin 0,028 kg/s kütlesel debi ile 16 Mayıs'ta olduğunu ve yaklaşık 0,82 ile 0,90'a ulaştığını, en düşük verimliliğin ise 06/Mayıs'ta 0,0055 kg/s kütlesel debiyle 0,57 ile 0,89'a ulaştığını göstermektedir. Suyun alıcıya geçerken birim zamanda absorbe ettiği faydalı enerji 1281,26 W' dır. Bu değer 0,028 kg/s debi ile Nisan ayında elde edilen en yüksek faydalı enerjiyi temsil etmektedir. Alıcıdan çıkan suyun en yüksek sıcaklığı 6 Mayıs tarihinde 0,0055 kg/s kütlesel debi ile 413 k'dir. 6 Mayıs tarihinde alıcıya geçerken birim zamanda suyun absorbe ettiği en düşük faydalı enerji 0,0055 kg/s kütlesel debi ile 1164,50 W' dır.

2023, 88 sayfa

Anahtar Kelimeler: Güneş enerjisi, Güneş ısısı, Isıl verim, Sıcaklık

PREFACE AND ACKNOWLEDGEMENTS

I would like to thank my thesis advisor, Prof. Dr. Halit ALTUNTAŞ, and Co-advisor, Prof. Dr. Yaseem H. MAHMOOD, for their patience, guidance and understanding.

Wisam Mohammed Fayyadh FAYYADH
Çankiri-2023

CONTENTS

LIST OF SYMBOLS

A_a	Aperture area
A_{col}	Surface area of the collector
A_r	Area of receiver
C_p	The specific heat capacity at a constant pressure of water
D_{in}	Internal diameter of the receiver
D_{outer}	The outside diameter of the receiver
I_a	The ratio of the sun's flux on the collector
I_b	Beam radiation
I_r	The ratio of the solar flow to the receiver
$\dot{m}$	Mass flow rate of water
Q_{loss}	Heat losses
Q_{opt}	Energy absorbed by the solar center
Q_u	Useful energy
CR_0	Optical Focus Ratio
CR_{max}	Maximum concentration
CR	Concentration ratio
d	Aperture diameter
f	Focal length
h	Depth of concentrators
h_r	Radiant heat transfer coefficient
h_w	Convection coefficient
I	Long-term average direct radiation
Nu	Nusselt number
p_{s_m}	Collector surface reflection
Q_{lc}	Heat losses by convection
Q_{lk}	Heat losses by thermal conductivity
Q_{lr}	Heat Loss by Radiation
Q_{out}	Useful energy
qu	Useful thermal energy
Re	Reynolds number
S	Shading Factor
t	Time
T_1	Temperature of heat transfer fluid entering the collector
T_2	Temperature of heat transfer fluid leaving the collector
T_a	Ambient temperature
T_{in}	The temperature of the water
T_{out}	The temperature of the water entering the solar collector
T_r	Mean temperature of receiver
T_w	Temperature of the water

U_L	Overall heat loss coefficient
V	The speed of air
α	Absorbent receiver
ε	Reflective surface emission
η	Instantaneous thermal efficiency
ηo	Optical efficiency
σ	Stefan-Boltzmann constant
τg	Absorbent tube permeability
ψ-rim	Rim angle
K	Thermal conductivity coefficient
υ	Air viscosity

LIST OF ABBREVIATIONS

CSP	Concentrated solar power
CSS	Conventional Solar Still
CST	Concentrated solar thermal
PLC	Programmable logic control circuit
SDC	Solar dish condensers

LIST OF FIGURES

LIST OF TABLES

1. INTRODUCTION

Pollution and global warming have increased worldwide due to fossil fuels (gas, oil, Etc.). Therefore, researchers have turned to renewable energies (clean energy), namely (solar energy, underground energy, wind energy, Etc.). For this, researchers have worked on designing and developing or advancing some parts of systems. Energy is an essential pillar in the economic construction of all countries, especially the industrial ones, where the amount of energy consumption has become an indication of the extent of progress of these countries due to its use in various fields. Therefore, the rationalisation of traditional energy consumption and the search for alternatives has become necessary not only for industrially developed countries but for all countries worldwide. Solar energy is one of these basic alternatives, as it has been used in producing electric energy, water desalination, and heating. It is also a partial alternative to conventional energy in the field of heating and cooling. The continuous progress in the various sectors has contributed to the increase in the demand for conventional energy to achieve comprehensive development. This has led to the interest of the whole world to search for inexhaustible non-traditional sources of energy no matter how much the demand for traditional energy increases, as well as avoiding the environmental pollutants that result from the use of traditional energy. The developed world has begun to pay attention to renewable energy.

1.1 Renewable Energy

The whole world is going through a countdown to depleting fossil fuels. The impact of human activities on global climate change has led to the emergence of new technologies known as renewable energies. These are those energies that are naturally generated and characterized as inexhaustible, available in nature, renewable, being clean, and their use does not result in any environmental pollution. They include (solar energy - wind energy - tidal energy). Renewable energies are preferable to traditional energy sources because of their low costs and local availability. In addition, they are clean energies that do not run out, unlike traditional energies that cause environmental pollution due to hydrocarbon emissions. Due to its continuous availability, the vast majority of renewable and widely used energy sources are wind and solar. The demand for renewable sources is expected to increase gradually from 2 % in 2008 to 50 % in 2050 due to the modern lifestyle that consumes many traditional sources. Figure 1.1 shows the increase in global demand for primary energy sources, according to the report presented by the International Energy Agency in France – Paris (Goswami 2022).

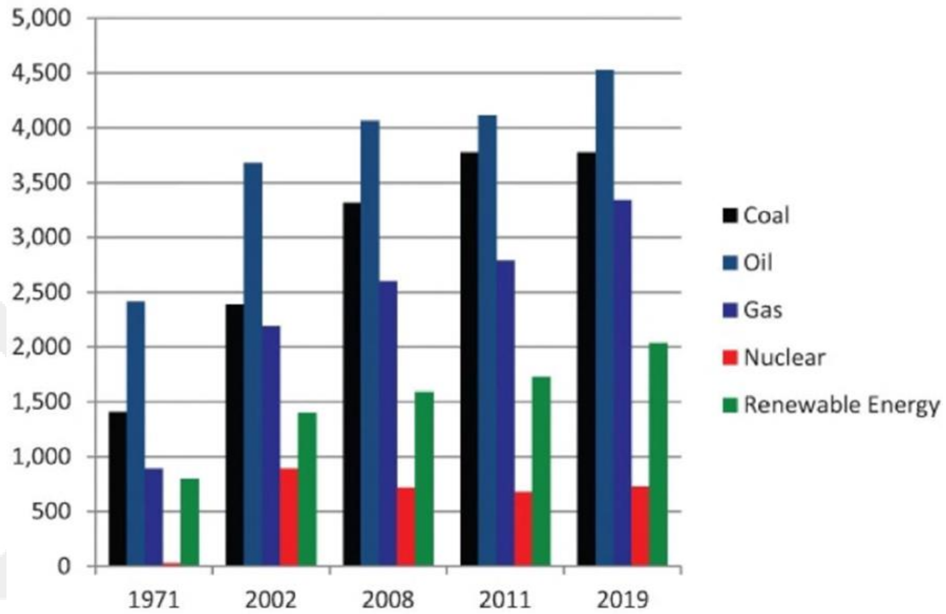

Figure 1.1 Data obtained from the International Energy Agency (Goswami 2022)

1.2 Solar Energy

Solar energy is one of the most important and widely used types of renewable energy due to its abundance and ease of use. Thus, it can be used as an important and effective alternative to traditional fossil energies. The amount of solar radiant energy that falls on the Earth's surface per unit area and unit of time is called radiation. It is estimated that the amount of radiation that continuously approaches the Earth's atmosphere is 1.75×10^5 terawatts, except that the atmosphere intercepts a large part of the solar radiation, i.e., the actual arrival is about 1.05×10^5 terawatts of radiation. Accordingly, it is shown that if only 1% of this solar radiation falling on the Earth could be converted into electrical energy with an efficiency of 10%, this would provide us with a resource base with a capacity of 10^5 terawatts. Considering that solar energy is one of the most important alternative energy sources that are widely and continuously available throughout the year in most countries, this has made it one of the essential energies used to generate electricity or employed for other uses, either directly through photovoltaic cells or indirectly as it is the case with concentrated solar power collectors. Solar energy plays an essential role in major industrial countries such as the United States of America and European countries towards meeting the industry's energy requirements. Moreover, solar energy has entered into several applications for concentrated solar collectors, and Figure 1.2 illustrates these applications (Sharma 2011).

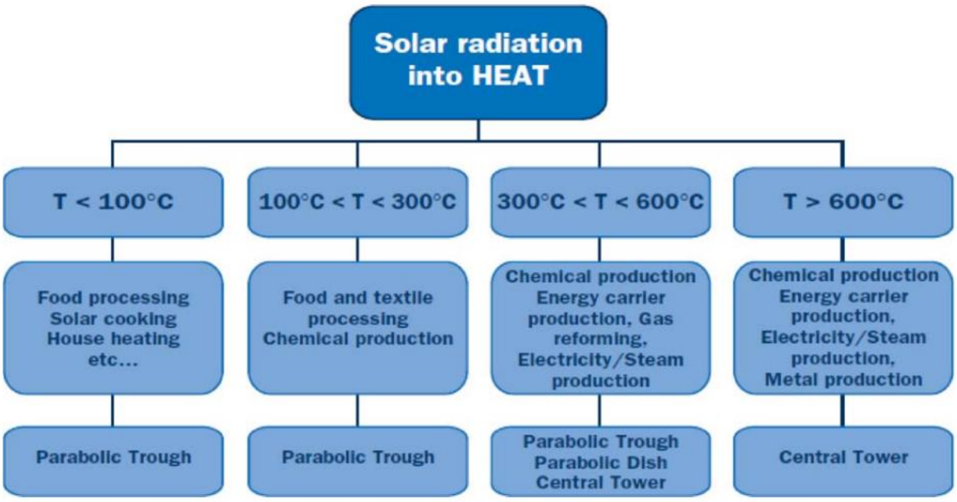

Figure 1.2 Applications for Concentrated Solar Power system (Sharma 2011)

Solar Thermal Energy: this is a carbon dioxide-free energy source. Solar thermal systems are relatively low maintenance due to their use of simpler technologies and passive systems that have no mobile parts. One of the most important solar thermal systems is solar energy heaters. Solar energy heaters are one of the most important solar energy applications. The solar heater exploits solar energy to heat water directly and not generate electricity, as with solar panels. Solar heaters have been present for over a hundred years. However, in the last two decades, the technology of solar heaters has developed significantly and remarkably, and most of the development has been in solar collectors. As shown in Figure 1.3, solar collectors can exploit more than 50% of the falling solar energy. Solar water heaters consist of four main components: the solar core, the receiver, the insulated tubes, and the hot water tank. Electronic controls can also be included, as well as a freeze protection system for cold climates (Bloess *et al.* 2018).

Figure 1.3 Solar heater

Solar energy is an alternative energy that is within reach of all human beings but has yet to be widely invested in. However, people have recently turned to renewable energy on a large scale, and nearly 20 % of the electric energy in the world depends on renewable energy (Duffie and Beckman 1980). The growth in renewable energy sources throughout the developed world is likely to rise to 33 % by 2040 as a result of population growth and thus leading to an increase in industrialization (European Union Commission 2012). The energy demand has increased dramatically. We can obtain renewable energy through natural resources such as (thermal energy, biomass, wind energy, solar thermal energy, Etc.). This has become the focus of most countries due to sustainability and the advantages of reducing carbon dioxide and greenhouse gas emissions. Among the technologies based on solar energy sources to produce energy are a technology that uses reflective materials (parabolic mirrors). This technology is part of the radiation focus category, where mirrors capture and focus the incident solar rays into the focal area where the receiver is located, which is usually next to an electric generator. Thus, solar energy is transformed into thermal energy in the receiver, mechanical energy in the engine, and finally, electricity in the generator (Edenhofer *et al.* 2011).

1.3 The Sun

The sun is the primary source of solar energy. It is the centre of the solar system, which emits energy and electromagnetic radiation at a significant and constant rate 24 hours a day and 365 days a year. The rate of what is emitted from this energy is equivalent to the energy produced by a furnace at a temperature of 5777 K. If it may be possible to obtain the incoming energy 100.000 m^2 from the surface of the sun, we can have enough of this energy to meet the current demands in the world (Duffie and Beckman 2013). The sun is a globular, glowing body with a high temperature, a diameter of 1.39×10^9 m, and an average distance from the earth of 1.5×10^{11} m. It rotates around itself once every four weeks, its temperature in the centre is 8×106 40 × 106 K, and its density is about 100 times greater than that of water. It is a continuous nuclear reactor maintained by the forces of gravity. The critical process is that hydrogen turns into helium by releasing enormous energy. The energy produced in the inner regions of the sun reaches temperatures of several million degrees, converted into radiation outside the surface and then into space, in which these emissions are electromagnetic spectrum radiation. Solar radiation can vary over time, so the maximum value of solar radiation is used when designing a system to determine the peak rate of energy input for that system. The designer needs to know the difference in solar radiation over time to improve the centre’s design, and the unit of measurement of sunlight is J/m^2, while in many cases, it is taken as W/m^2.

The continuous progress and growth of technology in various sectors, including (industrial, agricultural, military, and others), has led to the increasing demand for energy sources to achieve comprehensive development. This is what made man search for non-traditional sources of energy, permanent and not subject to depletion, no matter how much the demand for them increases, in addition to the environmental pollutants that result from the use of fossil fuels and other fuels (Răboacă *et al*. 2019). That is why humans have resorted to renewable energy, as it is the best solution for generating energy and preserving the environment. Among the most important types of renewable energy are solar energy, wind energy, hydro energy (dams), wave energy, tidal energy, bio-gas energy, geothermal energy, and other energies (European Union Commission 2012, Spelling 2011, Tauseef *et al.* 2013, Alwan *et al.* 2020). These are alternatives to fossil fuels to avoid emissions that could lead to the greenhouse effect and reduce dependence on fossil fuels, especially oil and gas (REN21 2008, Hosenuzzaman *et al.* 2015, Augustine *et al.* 2012).

Solar energy is the light and heat from the sun, which is invested using various methods such as solar heating, solar panels, and artificial photosynthesis. Solar radiation is regarded as one of the most important and widely used renewable energy sources. Solar energy is characterized as reaching all human beings in addition to being clean energy that can be benefited by generating electric power, water desalination, heating, and cooling. (Kabir *et al.* 2018).

1.4 Solar Concentrators

Solar concentrators are exchangers that have the ability to convert direct solar radiation into useful energy. The principle of its work is to focus the direct solar radiation falling on the reflective surface of the collector to the specific area known as the focus. The reflected radiation is collected at that point in the form of heat and then transferred by a heat transfer medium, which may be (air, water, or oil). The efficiency of solar collectors depends on the angle of inclination of each piece and the accuracy of the distribution of the mirrors. There are many designs that differ according to different applications (Zhu *et al.* 2015). There are several types of solar collectors, as shown below. (Strantzali and Aravossis 2016, Pandey *et al.* 2016, Răboacă *et al.* 2019, Mohammed 2013, Farret and Simões 2006). Raguram and Lingeswaran (2014) compared between a parabolic shaped dish collector that concentrates solar radiation to reach the temperature of 700 °C and another in the shape of a basin which uses heat to operate a Stirling engine. It is found that the dish is efficient and can be used as a heat source for a Stirling engine. Basem *et al*. (2022) studied the design and construction of a new system for generating electricity using solar energy. A parabolic solar dish is designed with a diameter of 3.0 m and an area of 7.1 m^2. It is equipped with a sun tracking system that allows movement on two axes whose primary function is to generate water vapor as an alternative to the steam boiler used in steam power plants. Several modifications are made to allow the new system to operate on the Rankine cycle system for power generation. The results show the success of the new system in generating electricity in the range of 800-1000 steam temperatures and reaching 400.1 °C with a total cycle efficiency between 32% and 42%.

1.4.1 Solar tower

It is a type of solar collector used to collect the energy of direct solar radiation. It consists of many planar reflecting mirrors of solar radiation (i.e., large individual tracking mirrors that can change orientation to track solar radiation) to focus the sun's rays on the top of the power tower, as shown in Figure 1.4. The towers rise from the ground tens of meters, and through the concentration of solar radiation by the mirror, high temperatures are obtained, which reach (1200ºC). The efficiency of these towers depends to a large extent on the quality of the performance of the mirrors, and the main aim remains, which is to collect the maximum amount of solar energy at the lowest cost. (Dafle and Shinde 2012, Zhu *et al.* 2015, Farret and Simões 2006).

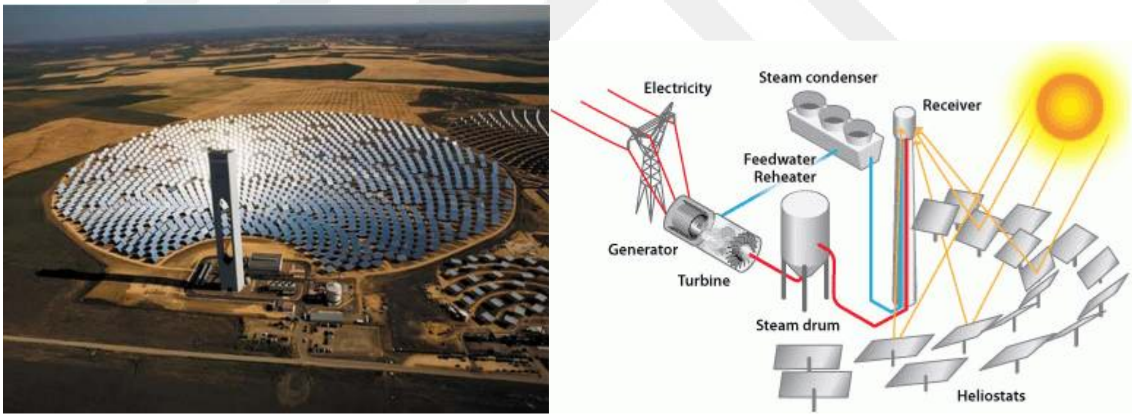

Figure 1.4 The power Tower Collectors (Islam *et al.* 2018)

1.4.2 Parabolic trough

These collectors take the form of a parabola, which collects the solar radiation in focus in the form of a line along the parabolic trough containing a tube to heat the water, as in Figure 1.5. The system with a larger design contains a rotating arc to track the sun only on the vertical axis, and the horizontal axis remains fixed from east to west (Farret and

Simões 2006). The oil absorbs heat inside the tubes that transfer heat energy to water in the heat exchanger.

Figure 1.5 A collector with a parabola form (Abbott 2009)

1.4.3 Parabolic dish collector

This type of collector is one of the most widely used solar collectors. It is often made of one piece or a combination of several pieces of mirrors and lenses and takes the form of a parabola, as shown in Figure 1.6. There are different designs and shapes of this type of collector, and the dish, resembling the one used to receive the television signal, remains the most widely used type. The dish is coated with reflective material or mirrors after cutting and pasting its entire area. Aluminium can be used as a reflective material that benefits from direct solar radiation as the centre collects it in a small area to produce high temperatures. The most important feature of this type of collector is that it can be equipped with a sun-tracking system with horizontal and vertical axes to track solar radiation from sunrise to sunset and from top to bottom. (Mohammed 2013, Farret and Simoes 2006, Zhu *et al.* 2015, Liu *et al.* 2016, Rajamohan *et al.* 2017). Mahmood *et al.* (2015) manufactured a two-meter-wide solar collector, and its surface was covered with pieces of mirrors to focus solar energy on a receiver placed in the focus to obtain boiling water of more than 100 °C, used for heating purposes. A tracking system was also used and a tank to collect hot water. Hijazi *et al.* (2016) designed a low-cost and medium-sized dish collector to generate electricity directly. This model can be installed in rural areas that are not connected to the government network and has three diameters (5, 10, 20) meters. He studied suitable dimensions of surfaces that reflect radiation and the type of metal available locally from the sheets available in the market, aiming to reduce costs and obtain good performance. Mahmood and Al-Salih (2018) designed two 2.0 m diameter solar dish condensers (SDCs) to heat water. This study applies to solar water heaters (SSWH). The interior surface of both dishes is reflective and coated with galvanized steel. The dish's first inner surface has a layer of reflectivity up to 80%, while the second has 95%-reflective mirrors. The receptors are placed at both plates' focal positions. Temperature and sun energy measurements for both kinds have been recorded. The first dish's light energy is 1909 W, the final energy is 1551 W, and the efficiency is 61%. The second dish's light energy is 1607.68 W, the final energy is 1853 W, and the efficiency is 73%. The results show that the materials used in this study are inexpensive and high-quality to make the solar condenser, but the dish coated with mirrors is superior and can heat water.

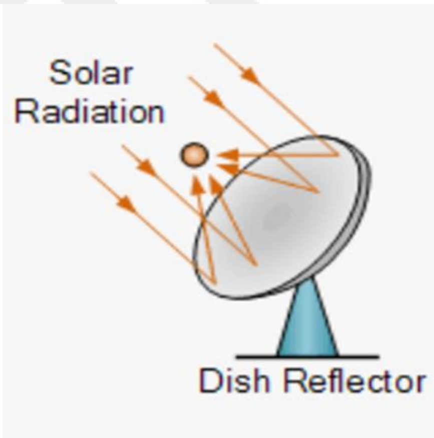

Figure 1.6 The Parabolic Dish Collector (Abbott 2009)

1.5 The Study Objectives

- ❖ Designing a parabolic dish solar centre to be used for the purposes of heating water, storing it in an isolated water tank, and using it for domestic purposes.
- ❖ Designing the solar centre in such a way as to reduce air resistance.

- Developing or improving of the tracking systems in order to receive more amount of solar radiation with lower cost.
- Obtaining a high-water temperature in a short time and with high heating efficiency.
- Finding the amount of gained energy inside the solar centre.
- Detecting the efficiency of the solar centre.
- Taking into advantage the intensity of thermal solar radiation.
- Reducing cost.

2. LITERATURE REVIEW

2.1 Radiological Properties

The sun is a valuable and effective source of solar radiation in the area of interest, so this must be considered when discussing solar energy utilization. How to get this energy and improve its use efficiency are what is needed. The issue necessitates the creation of technology for solar energy collection in order to gather the most significant quantity of energy at a fair price, as well as an extensive and accurate understanding of the interaction between the various areas on the earth and the sun. One of the most significant regions for solar energy investment is the Arab world, which includes Iraq.

2.2 Solar Spectrum

The sun is a gigantic nuclear reactor that constantly works to convert the nucleus of the hydrogen element into helium. The emission of huge amounts of energy in the form of electromagnetic energy accompanies the conversion process. The radiation travels long distances toward Earth or other planets (Howell *et al.* 1982). Electromagnetic radiation (EM) is a carrier energy through space. It is classified into two types based on the wave frequency: gamma rays of the smallest waves and radio waves of the longest ones, starting at 1 mm. In between these two limits, there are rays which are Infrared, visible, X-ray, ultraviolet, and microwave. The wavelength of the rays emitted by the sun is close to the shape of a black body with a temperature of approximately 5700 K. (Aden and Meinel 1977, Kalogirou 2004).

2.3 Radiological Properties

When the radiation hits the body, a part of this radiation is reflected while the other part is absorbed. If the material has a transparent specification, the radiation travels through it. The reflected incident radiation portion is defined as the reflection ρ, the absorbed portion as the absorption α, and the transmitted portion as the transmittance. When it comes to solar radiation, there are two types of radiation reflection, namely mirror and diffuse. Specular reflection occurs when the angle of incidence is equal to the angle of reflection, and the radiation is widespread when the reflected radiation is uniformly distributed in all directions (Kalogirou 2004).

2.4 Concentrates

To concentrate solar energy (direct solar radiation), the presence of a concentrator and a receiver (absorber) are needed. Therefore, concentrators are a mixture of mirrors, lenses, or coatings, which use to focus direct sunlight on the focal point. For the purpose of producing forms of useful energy Q_{out}, such as heat, electricity, etc., various techniques are used. The concentration ratio of these concentrates is given by dividing the area o Concentrator: - a device that re-converts the radiation falling on it to one area focus.

Concentrator: a device that re-converts the radiation falling on it to one area focus.

Geometric focus concentration ratio (CR): This depends on the collector aperture and receiver area, and it is given by Equation (2.1). (Thakkar *et al.* 2015, Mohamed *et al.* 2012):

$$CR = \frac{A_a}{A_r} \tag{2.1}$$

Optical focus concentration ratio (CR_O): It is the ratio of the solar flow on the receiver (I_r) to the ratio of the solar flow on the centre (I_a). The optical concentration ratio gives the actual optical losses resulting from the refraction and reflection of sunlight that occurs in solar collectors. In fact, it is used in calculations as it gives an insight into the thermal losses that occur in the receiver region, and it is shown by the Equation (2.2) (Teles *et al.* 2017):

$$CR_0 = \frac{I_r}{I_a} \tag{2.2}$$

Acceptance angle: Another property that concentration depends on is an acceptance angle (θ_a). It is the angular range in which all or some of the incident rays are accepted without moving the solar collector. There is an inverse relationship between the angle of acceptance and the percentage of concentration. If the percent ratio of the concentration is increased, the range of the acceptance angle is reduced. The maximum concentration that the solar collector can reach at the angle (θ_a) is so, that the collector accepts all the rays falling on it. The relationship is given by Equation (2.3) (Rabl 1985):

$$CR_{max} = \frac{1}{\sin^2(\theta_a)} \tag{2.3}$$

The main objective of using concentrates is to improve performance (increase efficiency) at higher temperatures by reducing heat loss as well as improving the economy by reducing costs (O'Gallagher 2008).

2.5 Receiver

The receiver is a black body which has the ability to trap incoming solar radiation by making use of cavities or tubular panels painted in black. A receiver can be defined as intercepting and absorbing concentrated solar radiation and converting it into usable energy. The task of choosing a receiver is complex as it depends on many factors including operating temperature, heat storage and thermodynamic cycle. The solar ray density of some types of receivers ranges between 300 to 1000 kW/m^2. There are many receivers that are used in solar thermal systems, but the most efficient is the cavity receiver. It is the most widely used because of its lower heat loss compared to other receivers. The optical performance of high-temperature solar thermal collectors is closely related to the size of the receiver. If the receiver is small and insulated by thermal fleece, the heating loss will be less (Luceno *et al.* 2021, Romero and Steinfeld 2012).

Madadi *et al.* (2014) investigated the effects of solar dish collector receptors. A solar dish with a diameter of 2.88 m, two types of conical and cylindrical receivers with three different diameters (0.2,0.12,0.05 m) and (0.2,0.14,0.115 m) respectively to test the influence of receiver aperture on system performance. Heat transmission between the receiver and the sun accounts for 35% to 60% of energy losses. Fully opened receivers have superior thermal efficiency and energy. The cylindrical receiver's lower energy losses make it more energy and heat efficient than the conical receiver. The same applies to the drop hole. Rajamohan *et al.* (2017) developed a novel solar water heating system technology. A parabolic dish condenser, conical heat sink, and water heater make up the solar water heating system. Due to its light weight and simplicity of production, aluminium sheets are used to make the parabolic plate assembly. Quality 2.0 mm mirror glass with 95% reflectivity was used. New solar water heating technology is the focus of this research. A parabolic dish condenser, cone-shaped absorber, and water heater made up the new solar system. In this system, the conical absorber directly absorbs solar radiation from the sun and the parabolic dish condenser reflects it from all directions.

Swanepoel (2019) examined the performance of the solar collector (solar reflector and solar receiver) under actual sun thermal conditions, which consists of six Mylar sheets stretched over satellite dish elliptical edges. Mylar faces reflect 97% of visible light. 135 mm receiver hole diameter has an 87% cross factor. The thermal test is done on a sunny, calm day. Over the day, the solar collector tracked the sun with a 1-degree inaccuracy. The receiver's temperature and pressure are measured when municipal water passes through at 0.284 g/s. The entrance temperature was 54 °C and the output temperature was 343 °C during a 91 minute test. Solar radiation dropped from 801 to 705 W/m^2 throughout this test. The aperture intercepted radiation has lowered from 1,845 to 1,625 watts using a 2.73 m^2 reflector. During the test, the working fluid input averaged 861 W and heat loss ranged from 1,000 to 750 W. Heat loss research shows that the aperture loses 84% of heat, with 31% from reflected radiation.

Research by Charran (2020) aims to provide a new "visual evidence" for improving the performance of conventional thermocouples and receivers in parabolic solar collectors for use in a home solar water heater with the integration of a PCM latent heat storage module. Two ray-tracing programs were used, Sol Trace TM and Tracer TM. Sagada *et al.* (2021) used a hand-held parabolic dish solar geyser (PDSG) to instantly generate hot water in the home and small commercial settings. For this purpose, the solar geyser is tested for its thermal performance using three different flow modifiers and configurations of the cut conical receiver (hollow coil). Experimental results show that the proposed solar geyser can instantly generate hot water with sufficient temperature (~50-60°C) for immediate consumption. Swanepoel *et al.* (2021) tested a low-cost helical-coiled cavity receiver and a prefabricated solar condenser to create steam at water pressures above 3 bar. Working fluid temperatures and pressures are monitored throughout the coil. The working fluid caught 861 W of heat with an output temperature of 343 °C and an average solar radiation of 757 W/m^2 using a 2.70 m^2 condenser and 0.294 g/s water flow. The collector and receiver averaged 42% and 50% thermal efficiency during the test. Second law efficiency averaged 12%. Temperature variations between the coil surface and the working fluid reveal flow patterns.

Hassan *et al.* (2021) examined energy, strain, and optical performance of two parabolic solar dish condenser cavity-type acceptors. Water flows at 0.83 litters per minute via the cylindrical and conical tube receivers, which are developed and tested at 35°C to 190°C. The conical tube receiver is best, followed by the cylindrical form. The conical hollow tube design offers 62% average thermal efficiency, 11% external energy efficiency, and 82% optical efficiency under 865 W/m2 solar radiation. From the slack meter, the cylindrical and conical cavity receivers had total heat loss coefficients of 137 W/m^2 and 125 W/m^2, respectively. Both cylindrical and conical tube receptors had maximum and mean surface temperatures of 140, 115, 155, and 125°C. COMSOL Multiphysics is used to simulate receiver temperature dispersion. The high-capacity lightweight conical tube receiver powers water heating applications with a parabolic dish concentrator. Kasaeian *et al.* (2021) review prior work on cavity receiver geometries and parabolic dish collector improvements. This document examines cylindrical, hemispherical, conical, and flat cavity receivers. The conical bore form has 70% thermal efficiency, 30% external energy efficiency, and 87% optical efficiency at 200°C. Solar dish collectors typically operate at 650–750 °C. Due to the greater operating temperature and cavity shape, heat losses such radiation, conduction, and convection might reduce system thermal efficiency. Diameter ratio, cavity inclination angle, tube type, and tube form can also affect cavity heat loss.

Pawar and Tungikar (2022) used a 16 m^2 Scheffler parabolic dish condenser to test the thermal performance of the helically coiled conical cavity receiver under radiation circumstances. The receiver's thermal energy efficiency, external energy efficiency, and heat transfer coefficient are studied under three radiation situations. The receiver is tested at 2.5 litters per minute with water as a heat transfer fluid at 30-100°C. For 654 W/m^2 incoming beam radiation, the receiver's maximum stagnation temperature is 395°C, indicating its capacity to create pressured vapor. Slack test heat loss coefficient is 116 W/m^2K. The receiver power and energy efficiency are affected by heat transfer fluid input and output temperatures and incoming beam radiation. The second experiment's highest radiation 672 W/m^2 yielded 70.20% thermal energy efficiency and 8.69% energy efficiency. According to the data, this receiver can create steam under pressure at temperatures over 100°C.

Optical energy: is the rate of light energy absorbed by the receiver (metal) from the solar centration using the Equation (2.4) (Mohamed *et al.* 2012):

$$Q_{opt} = A_a \ \rho_{s\_m} \ \tau_g \ \alpha_r \ S \ I_b \tag{2.4}$$

Where:

- A_a: area of the reflective surface
- ρ_{s_m}: reflectivity of the collector surface
- τ_g: transmittance of the glass
- α_r: absorbance of the receiver
- S: receiver shading factor
- I_b: solar radiation falling on collector

Thermal losses (Q_{loss}): They are the losses resulting from the receiver. They can be calculated by detecting the area of the receiver (A_r) with the total loss factor (U_L) and finding out the mean or average temperature of the receiver (T_r) and the ambient temperature (T_a). This is given by the following relationship Equation (2.5) (Duffie 1991, Alarcon *et al.* 2013):

$$Q_{loss} = A_r \, U_L \, (T_r - T_a) \tag{2.5}$$

The average receiver temperature is obtained by Equation (2.6):

$$T_r = \frac{T_{out} + T_{in}}{2} \tag{2.6}$$

The coefficient of total heat loss is given by the following Equation (2.7):

$$U_L = [\frac{1}{h_w - h_r}]^{-1} \tag{2.7}$$

where:

- h_r: Radiant heat transfer coefficient
- h_w: Convection heat transfer coefficient.

The radiant heat transfer coefficient can be given by Equation (2.8) (Alarcon *et al.* 2013):

$$h_r = 4 \; \sigma \; \varepsilon \; T_{mean}^3 \tag{2.8}$$

where:

- ε: is the emissivity of the receiver
- σ: is a constant Stefan-Boltzmann ($5.67 * 10^{-8}$ W/m^2 K^4)

The convective coefficient h_w can be given by the following Equation (2.9):

$$h_w = \frac{k_{air}}{D_{outer}} \ . \ Nu \quad (2.9)$$

The appropriate equation for calculating the Nusselt number (Nu) depends on the Reynolds number for air (Re) according to the following:

Nu is given by Equation (2.10) and Equation (2.11):

$$Nu = 0.40 + 0.54 \ Re^{0.52} \quad (2.10)$$

$$Nu = 0.30 \ Re^{0.6} \quad (2.11)$$

Reynolds number (Re) is given by Equation (2.12):

$$Re = \frac{V \ . \ D_{outer}}{v} \quad (2.12)$$

where:

- V: is the speed of air (m/s)
- v: is air viscosity 5.15×10^{-5} m^2/s

If 0.1 < Reynolds number <1.000, then Equation (2.10) is used.

If 1,000 ≤ Reynolds number <50.000, then Equation (2.11) is used.

2.6 Total Heat Losses for the Receiver

The total thermal losses in the receiver are due to the effects of the three basic heat transfer mechanisms: conduction thermal losses Q_{lk}, convection Q_{lc}, and radiation thermal losses

Q_{lr}. The total thermal losses are given by Equation (2.13). (Al Hamadani 2019, Günther *et al.* 2011, Loni *et al.* 2022, and Bissert *et al.* 2016).

$$Q_{loss} = Q_{lk} + Q_{lc} + Q_{lr} \quad (2.13)$$

2.6.1 Heat loss by radiation

The process of heat loss by radiation from applications with high temperatures is more important than heat loss by convection and conduction. This is due to the fact that heat loss by radiation is directly proportional to the difference in temperature to the fourth power and surface emission according to Stefan-Boltzmann law, which is given by the following Equation (2.14):

$$l = \varepsilon . \sigma . T^4 \quad (2.14)$$

Whereas, the heat losses by convection and conduction are linear, concerning the difference in ambient temperature and receiver temperature. The radiant heat loss increases as the temperature is higher than the heat loss by convection and conduction. These radiation losses are reduced by reducing the receiver area and increasing the receiver absorption. The Equation (2.15) for heat losses by radiation is given by:

$$Q_{lr} = h_r A_r (T_r - T_a) \quad (2.15)$$

2.6.2 Heat loss by convection

Convection occurs either due to wind, and this type is called forced convection, or because of the difference in temperature between the receiver surface and the surrounding air. Both types of convection depend strongly on the direction of the receiver, and this is shown by the following Equation (2.16) (Loni *et al.* 2022):

$$Q_{lc} = h_w A_r (T_r - T_a) \quad (2.16)$$

2.6.3 Heat loss by conductive

Thermal conduction: It is transferring heat from an object which has a higher temperature to another object of lower temperature. Heat loss by conduction in solar collectors is due to the properties of the metal used, the thickness of the material, and its cross-section. Thermal losses due to heat conduction are less compared to heat losses due to radiation or convection. These losses are reduced if the receiver is covered with an insulating material. It is given by the following Equation (2.17) relationship:

$$Q_{lk} = k \ \Delta x \ A_r \ (T_r - T_a) \tag{2.17}$$

where:

- Δx: represents the rate of change in the thickness of the metal
- k: is the conductivity coefficient (W/m K)

2.7 Useful Energy

The amount of useful energy produced by the solar collector is determined by Equation (2.18) via substituting Equations (2.4) and (2.5) into the useful energy equation (Kadri and Abdallah 2016):

$$Q_{out} = Q_{opt} - Q_{loss} \tag{2.18}$$

2.8 Concentrator Efficiency

The obtained instantaneous efficiency of the solar thermal collector can be defined as the ratio of the useful energy received Q_{out} to the incoming solar energy Q_s. The absorption of solar energy rays in the solar collector depends on many factors or parameters, such as the size of the solar collector - the angle of the direction of the solar collector - the weather condition, and other variables that affect the efficiency (thermal, optical, instantaneous) of the solar collector. Thermal efficiency means (the ratio between the useful energy Q_{out} delivered and the solar energy falling on the centre hole (Q_s), as this energy is proportional to A_a and with I_b. The incoming solar energy Q_s is given by the following Equation (2.19) (Wu *et al.* 2010, Ahmadi *et al.* 2018):

$$Q_s = I_b \ A_a \tag{2.19}$$

where:

- I_b: solar radiation
- A_a: area of the concentrates

Thermal efficiency is a function of the temperature of the inlet and outlet water from the receiver as well as a function of the water flow rate and is given by the following Equation (2.20):

$$\eta_{collector} = \frac{Q_{out}}{Q_s} \tag{2.20}$$

The useful heat (Q_{out}) is related to the flow rate ($\dot{m}$), the specific heat at constant pressure (C_p) and the inlet and outlet temperatures (T_{in} and T_{out}) This is shown by the following Equation (2.21):

$$Q_{out} = \dot{m} \ C_p \ (T_{out} - T_{in}) = \dot{m} \ C_p \ \Delta \tag{2.21}$$

2.9 Parabolic Geometry

A solar dish is a symmetric parabola, and a parabola is the position of points in that plane that are equidistant from the guide and focus. The only parameter that defines a circular, not oval, geometry is a perfectly equivalent geometry as shown in Figure 2.1. This is given by the following Equation (2.22):

$$x^2 + y^2 = 4\ f\ z \tag{2.22}$$

where:

f: is the focal length

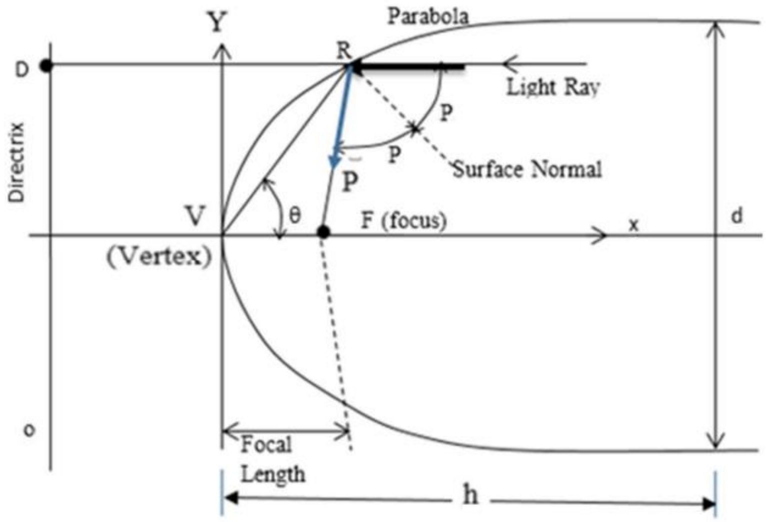

Figure 2.1 Parabolic curvature (Aliyu *et al.* 2021)

The basic characteristic to design the equivalent solar centre is the surface area, which can be estimated by considering (y= d/2 and h= x in) as shown in Figure 2.1. This is given by the following Equation (2.23).

$$S = [\frac{d}{2\sqrt{\frac{(4h)^2}{(d)^2}+1}} + 2\ f\,\text{In}[\frac{4.h}{d\sqrt{\frac{(4h)^2}{(d)^2}+1}}] \tag{2.23}$$

Concentrator area (A_a): It is the surface area of the stratigraphic concentrator on which solar energy falls. In other words, it is the area that receives solar radiation and can be calculated by the following Equation (2.24) (Newton 2007):

$$\text{A Concentrator surface area} = \frac{2\ \pi}{3\ P}\ [\sqrt{(\frac{D^2}{4} + P^2)^3} - P^3] \tag{2.24}$$

where $P = \frac{D^2}{8\,H}$, Equation (2.25)

$$\text{A Concentrator Aperture area} = \pi \,.\, (\frac{D}{2})^2 \qquad (2.25)$$

Receiver aperture area A_r: Whenever the aperture area increases, the losses which are due to heat transfer by convection and radiation increase. The aperture of the receiver can be calculated using the following Equation (2.26):

$$A_r = \pi \;\; R^2 \qquad (2.26)$$

The indicator of the arc of the parabolic receiver can also be called the rim angle. The larger rim angle of the parabolic dish can be divided into a steeper slope as shown in Figure 2.2. Equation (2.27) is used to find this angle (Günther *et al.* 2011, Mohamed and Eltahir 2013):

$$\text{Tan}\ \varphi\ \text{rim} = \frac{1}{\frac{d}{8\,.h} - \frac{2\,.h}{d}} \qquad (2.27)$$

f is the focal length and is given by the following Equation (2.28):

$$f = \frac{d^2}{16\,.h} \qquad (2.28)$$

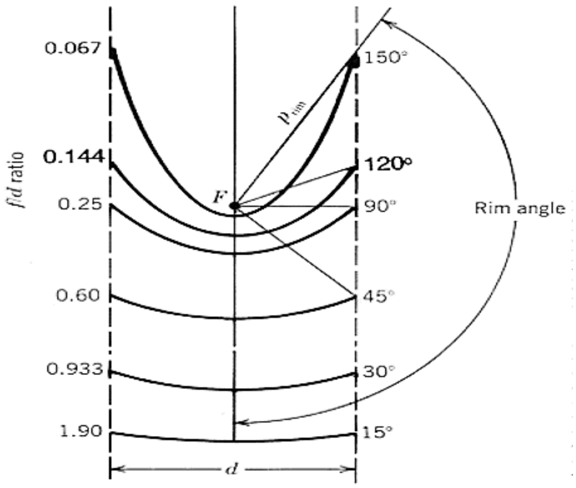

Figure 2.2 The edge angle and focal length of a fixed-diameter reflector (Al Hashmi 2015)

2.10 Intercept Factor

The section of the solar radiation which is reflected from the collector that hits the aperture is known as the intercept factor. This factor is inclined by the aperture's size, error of the dish system, rim angle, and other reasons which are not parallel with sunlight. The small energy that enters to the receiver can be increased by increasing the intercept factor. Increasing the intercept factor can also reduce the error of the reflection collector and improve system performance.

2.11 Energy Storage

Solar energy is one of the most promising renewable energies but faces some difficulties or challenges when used in the production of thermal energy. One of these difficulties is that the production of thermal energy from solar collectors is intermittently at sunset as well as when there are clouds. Therefore, to solve this problem, a thermal storage system is used. This stores the heat energy produced during the day and uses it at night. The storage system for this thermal energy must be highly efficient for later use when needed. The basic principle of storage is a simple one, as the generated thermal energy is collected by solar collectors and this energy is sent to a heat exchanger. This in turn leads to heating the fluid from the cold tank to the hot tank so that this energy can be recovered and used.

There are three main factors that must be considered when designing a thermal storage system in solar collectors: technical characteristics, cost-effectiveness and environmental impact. The technical characteristics are intended to increase the efficiency of the solar collector by increasing the high thermal storage capacity. Moreover, it maintains a good heat transfer rate between the heat storage material and the working medium. The cost-effectiveness is determined by the heat storage and heat exchanger materials and is closely related to the technical characteristics mentioned above (Kumar and Shukla 2015, Tian and Zhao 2012). There are several ways to store heat in solar collectors as illustrated in Figure 2.3 below.

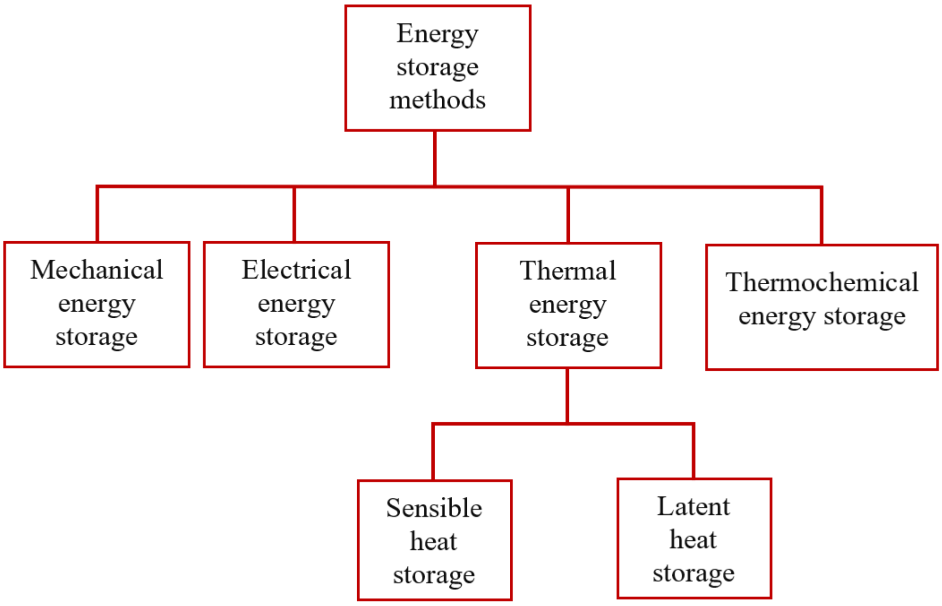

Figure 2.3 The different methods of energy storage (Kumar and Shukla 2015)

2.11.1 Apparent heat storage

Apparent heat: It is the storage of heat in a substance of mass ($\dot{m}$). The heat capacity (C_p) at the storage temperature is raised from (T_1 to T_2) as in the Equation (2.29) below and (p)is the density of the substance(kg/m^3) (Al Hashmi 2015).

$$Q = \dot{m} \int_{T1}^{T2} C_p \; dT = v \int_{T1}^{T2} p \; Cp \; dT = \dot{m} \, C_p \, dT \qquad (2.29)$$

The most common materials for heat storage are (water, molten salts, rocks, ceramics, and organic oils). However, water is most common for apparent heat storage with low- or medium-temperature solar systems. Like every method, there are advantages and disadvantages. One of the disadvantages of this method is that at high temperatures there is no temperature difference for the process of charging and discharging energy for the material used, and the reason for this is that these used materials do not change in phase or state. The other drawback, as mentioned earlier, depends on the mass, heat capacity, and high temperature of the material used. This leads to the storage of a relatively small amount of thermal energy, and in return a larger volume of materials used for storage is needed.

2.11.2 Latent heat storage

Thermal energy can be stored as latent heat in a material that undergoes a phase transformation at temperatures suitable for the application (T_m) if the temperature of the material is heated from (T_1 to T_2). Here, the thermal energy is stored in a material of mass ($\dot{m}$). The latent heat is given in the Equation (2.30) below (Al Hashmi 2015):

$$Q = \int_{T1}^{T2} \dot{m} \; Cp \; dT + \dot{m}\lambda + \int_{Tm}^{T2} \dot{m} \, Cp \, dT \qquad (2.30)$$

where:

λ: is the heat of transformation of evolution

The following Figure 2.4 shows the basic parts of the thermal storage system in solar thermal collectors. Also, the following Figure 2.5 shows the basic work principle of solar thermal concentrators

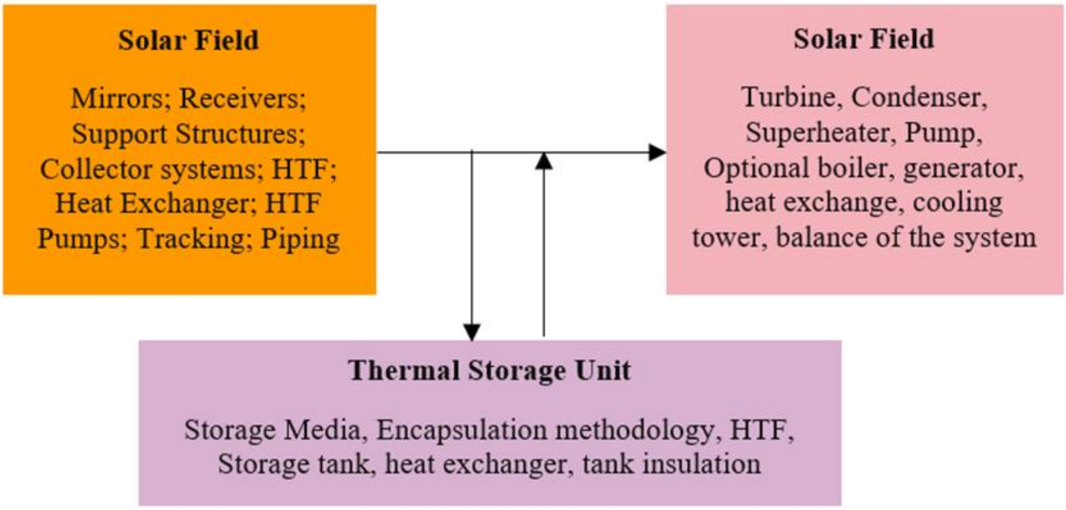

Figure 2.4 Thermal storage system in solar collectors (Islam *et al.* 2018)

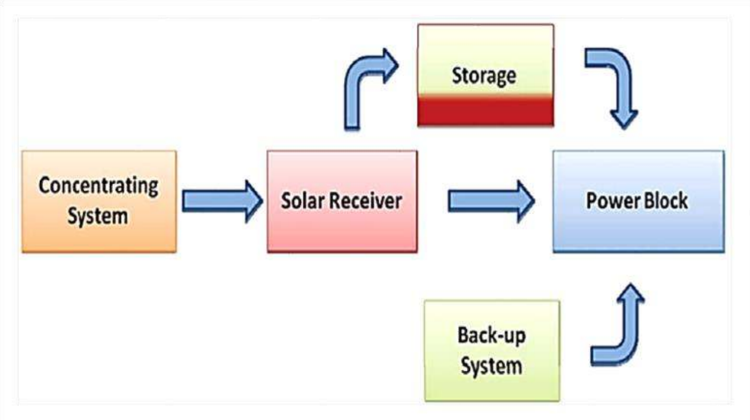

Figure 2.5 The working principle of CSP (Baharoon *et al.* 2015)

2.12 Sun Tracking

The solar collector that has point-focus needs direct sunlight. This tracking uses an electric motor and solar energy sensors to obtain the maximum amount of sunlight possible. Solar tracking has several benefits, including the ability to obtain solar energy throughout the day. The greatest energy per unit area increases the daily efficiency of the solar collector. There are many ways for tracking as in the following (Jin *et al.* 2013, Patil *et al.* 2016). Mohammed (2012) conceived and constructed a dish that follows the sun to heat water using solar energy utilizing an autonomous electronic control circuit with a hydraulic arm, light-sensitive circuit, and electric motor. The Nigerian investigation found that the solar heater worked well. The thermal efficiency is 52% to 56%, greater than projected, due to the adoption of an autonomous tracking system, which is superior to human tracking. Mohammed and Bartholomew (2012) compared the thermal performance of a dish solar collector's manual and electric motor tracking systems. The automatic method produced more than 2% thermal efficiency in less than 4% time, outperforming the manual system. An applied hybrid (modified) SDC solar collector and a basic CSS solar collector were compared by Omara and Eltawil (2013). The solar dish is wrapped with mirrors using a two-axis tracking mechanism based on a PLC. A black rubber line with round coils heats the water before reaching the receiver. The SDC and CSS efficiency rates are 68% and 34%, respectively. They also found that the hybrid solar collector's distilled water productivity was 347% higher than the regular solar collector's 244%. Mohammed (2013) created a basic, low-cost solar cooker. The cooker consists of a solar dish with a diameter of 1.8 m^2 and a depth of 0.29 m^2 coated with a sheet of reflective paper (polymer) with a focal length of 0.698 m that follows the sun by hand. The solar cooker is satisfactory and can cook 3 kg of rice in 90 to 100 minutes. Majeed *et al.* (2021) developed a solar parabolic dish and algorithm tracking system to monitor a water heater utilizing a dual axis time tracking method. A fixed parabolic solar dish (FPSD) and a tracking one are used to test two solar water heater types (TPSD). Water heating and two-axis sun tracking control systems make up the experimental arrangement. This study shows that Dual tracking technology increased heat exchanger water temperatures by 20% (TPSD is 20% higher than FPSD). TPSD and FPSD water temperatures peak around 1:00 PM at 50.8 °C and 47.3 °C, respectively. The TPSD model generates energy all day. At 1:00 pm, the maximum value is 71.06 W, whereas the FPSD model records 56.4 W.

2.12.1 Passive tracking method

In this method, control devices such as motors and others are not used. This depends on the thermal expansion of the materials or the pressure imbalance between two points at the two ends of the tracker. The partial heating method of two connected tubes filled with gaseous cooling is used as shown in Figure 2.6.

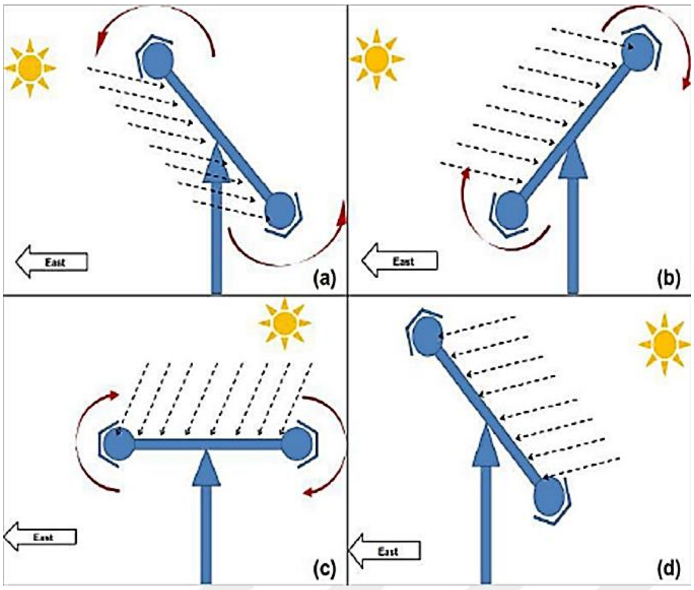

Figure 2.6 Explains how passive sunlight tracking works (Hafez *et al.* 2018)

2.12.2 Active tracking method

In this method, controllers are used, and are categorized into uniaxial and dual axis tracking. Uniaxial is tracking the sun daily from east to west or from north to south. In dual axis, both directions are used at the same time which is the best way to get the maximum amount of solar energy.

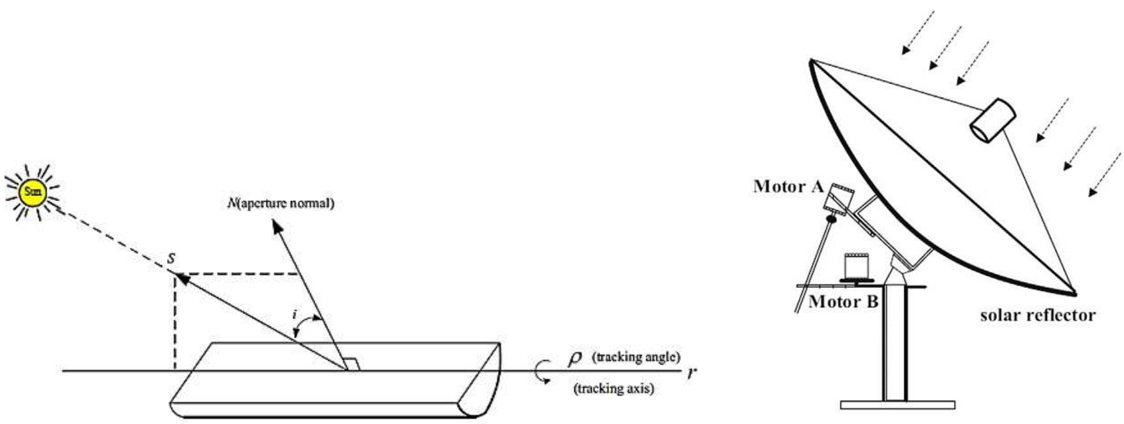

Figure 2.7 Left - Biaxial tracking method for a solar dish (Hafez *et al.* 2018), Right - Uniaxial tracking method for a parabolic solar trough (Wang *et al.* 2016)

3. MATERIALS AND METHODS

3.1 Introduction

Solar energy is promising for many countries due to the large amounts of solar radiation that reach the Earth. Solar energy consists of many technologies that are used to heat water. Among the best of these technologies are the dish solar collectors in terms of high efficiency, low cost, and ease of use. This chapter includes the practical part of the study and comprehensively describes the parts that make up the solar heater system with a solar dish concentrator. This chapter also shows how to design and manufacture the system. Moreover, it includes a detailed explanation of the manufacturing of the concentrator and the practical experiments conducted in this study.

3.2 System Mechanical and Electrical Parts

The system consists of two parts, Mechanical and Electrical parts, as shown in Figure 3.1 below.

Figure 3.1 Experimental system setup

3.2.1 Mechanical parts

3.2.1.1 Solar dish

Concentrating solar collectors are needed to obtain the necessary high temperatures due to solar radiation being a relatively low heat source. The selected type is the parabolic dish type as shown in Figure 3.2. The parabolic dish is a satellite dish with a diameter of 1.4 m and a depth of 0.14 m, obtained from local markets. The dish has been smoothed and painted white. The dish has a surface area of 1.599 m^2, an aperture area of 1.5386 m^2 and a focal length of 0.875 m.

Figure 3.2 Concentrator before modification (left), and after modification (right)

3.2.1.2 Reflective surface

The reflective surface consists of a square-shaped mirror, the length of the sides of which is 2 cm, and a reflectivity of 95% to reflect the solar radiation falling on the concentrator to one place, which is the focus. The mirror is fixed to the surface of the concentrator with a heat-resistant adhesive. Figure 3.3 shows the concentrator before and after installing the mirror pieces.

Figure 3.3 Solar collector with mirrors ben installed

3.2.1.3 Receiver

A stainless-steel cylindrical receiver is used consisting of two iron cylinders. The length of the first cylinder is 0.23 m, its inner diameter 0.152 m and thickness 0.007 m. The second cylinder is of the same metal with an inner diameter of 0.095 m and a height of 0.23 m. The two cylinders are closed from the back by a metal disc with the same thickness and fixed by welding with two holes of the diameter 0.00952 m for passing into the copper pipe. The front end is also welded, and a circular hole is made with a diameter of 0.095 m in the centre to match the location of the focal point. A copper pipe with a length of 12.5 m and a diameter of 0.00952 m is arranged in the form of a spiral coil and wrapped around the surface of the second roller. The receiver is installed (boiler) on the concentrator by using 3 steel rods in which the length of each rod is 1.20 m. The receiver is encased in insulating material (thermal wool) to prevent the loss of heat from the receiver to the external environment, except for the front aperture of the receiver (boiler) to allow solar radiation to the receiver. Figure 3.4 shows the receiver (boiler) and (k-type thermocouple) sensors. The images for the entire system are shown in Appendix 1.

Figure 3.4 Receiver setup on the dish

3.2.1.4 Solar dish base

The solar dish base consists of two parts, as shown in Figure 3.5. The first part consists of a tube with an outer diameter of 0.06 m and a length of 1.20 m. A flat base is connected to it from the top. Two bearings are installed at the top of the flat base. The bearings are connected to a circular disc, and the disc is connected to the concentrator from the bottom. The bearings are used to control the up-and-down movement of the concentrator via an electric motor, as shown in Figure 3.5. The second part consists of a tube with an inner diameter of 0.14 m and a height of 0.45 m. Two bearings are installed inside the tube, one at the top and the other at the bottom. The first part (the first tube) is installed inside the slot of the inner bearings so that its movement can be easily controlled by rotating to the right and left. This is performed via a serrated disk mounted on the first part (first pipe) connected to the moving part in the second part through an electric motor. A serrated tape manufactured from carbon steel metal. The dimensions of the tape are 0.50 m in length, 0.06 m in width, and 0.004 m in height. It is cut and manufactured by a laser device as shown in Figure 3.5. The function of the serrated tape is to engage and interlock with the serrated disk, as illustrated in Figure 3.5. the base is installed on a level surface. The images for the entire system are shown in Appendix 1.

Figure 3.5 Solar dish base

3.2.1.5 Solar dish base

Connecting pipes between the receiver and the water tank are used. The pipes are made of heat-resistant plastic material. The pipes are insulated with insulating material (thermal wool) to prevent heat loss. (To reduce heat loss between tank and boiler).

3.2.1.6 Water tank

The water tank is made of stainless steel, externally insulated with thermal foam and covered with aluminium foil to prevent heat loss. The tank has several entrances and exits, including an inlet and outlet for water at the bottom of the tank to feed the receiver with water through the pump. In the water tank, there is a point where the water goes to copper coils, an entry point where the water is transferred back to the tank. There are also two apertures in the tank; one is at the top, through which the tank is filled with water and the second in the middle, through which a k-type sensor is placed. Figure 3.6 shows the water tank, the temperature sensors, and the mass flow rate meter.

Figure 3.6 Water Tank

3.2.2 Electrical parts

3.2.2.1 Pump

Water is supplied to the receiver from the tank using a pump. There is a water pump point from the tank to the copper coils, and the pump is equipped with a flow meter installed to monitor and adjust the flow rate. A valve is placed before and after the pump to adjust the flow rate, and a valve is placed before the water enters the tank. Figure 3.7 shows the water pump.

Figure 3.7 Water Pump

3.2.2.2 Tracking system

A tracking system is employed by using an Arduino device and a Relay as a control device to control the DC developers in order to control the bases of the solar dish with a vertical axis. This is conducted to move the dish from bottom to top with the rising of the sun disk accompanying the movement of the dish from east to west and vice versa, as shown in Figure 3.8 below.

Figure 3.8 Arduino control system (left) and relay system (right)

3.3 Measuring Devices

Certain scientific devices are used to measure the scientific variables of the experiment, and among these devices are:

3.3.1 Solar power meter

The solar power meter sm206-solar device is used. It is an easy-to-use solar radiation measurement device. The sensor is directed toward the sun. Thus, the solar radiation is vertical on this device and measured from morning to sunset. Readings are recorded over time. The radiation is measured by the unit W/m^2, as shown in Figure 3.9.

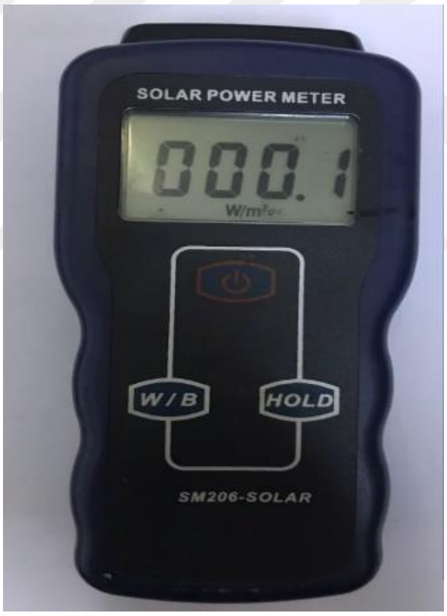

Figure 3.9 Solar radiation measurement device

3.3.2 Temperature measurement device

The k-type thermocouple device is used, as shown in Figure 3.10. As shown in Figure 3.10, seven thermal sensors are used in the system. There are three in the water tank at the waterproof exit and the waterproof entry into the tank, with the third-placed in the middle of the tank. The other four are used when the water comes in and out of the boiler, with the third in the boiler in the middle and the last outside the boiler.

Figure 3.10 Temperature measuring devise (left) along with the thermal sensors k-type (right)

3.4 Experimental Works

3.4.1 Measuring the engineering properties of the solar system

The engineering properties of the collector are measured, focal length (f), rim angle, parabola aperture diameter (d), parabola depth (h), concentrator aperture area, and the solar concentrator area. This is conducted via employing Equation (2.1), Equation (2.24), Equation (2.25), Equation (2.26), Equation (2.27) and Equation (2.28).

3.4.2 Measures of solar radiation

Solar radiation is measured on different days of April and May using a device of the type (solar power meter sm206-solar) as shown in Figure 3.9. Readings are recorded starting from nine in the morning until six in the evening.

3.4.3 Measures of receiver temperature

The receiver's temperature is measured without water. The receiver is placed in the focus through the solar tracking so that all the falling solar rays are in the parabola concentrator towards the receiver aperture (the focus). This raises the temperature of the receiver before entering the water. The measurement is taken by means of the thermal sensors (i.e., sensors of the k-type receiver) via a small hole located in the receiver's base.

3.4.4 Measures of water temperature

The temperature of the water entering the receiver and exiting it is measured hourly from nine in the morning until six in the evening using a (k-type thermocouple) device. The temperature of the water entering and exiting the water tank with the air temperature surrounding the work area are measured.

3.4.5 Measures of mass flow rate

The mass flow rate from the tank to the receiver is measured using a mass flow meter. The flow rate is controlled by placing three valves, two between the pump and the receiver and the third between the receiver and the water tank. The function of these valves is to control the flow rate.

3.4.6 Heat transfer process

By knowing the engineering properties of the system with the conversion of solar radiation into heat, the working fluid (water) is heated. It is possible to detect the optical power, thermal losses, and useful power through detailed knowledge of the engineering properties of the collector and receiver.

3.4.6.1 Optical energy

By finding the optical properties of both the collector and the receiver, the optical energy (Q_{opt}) can be found through employing Equation (2.4).

3.4.6.2 Thermal losses (Q_{loss})

By knowing some properties and data such as wind speed, air temperature, receiver diameter, average receiver temperature, and the heat loss coefficient U_L, which in turn depends on the linearized radiation coefficient (h_r) and the convection coefficient (h_w), the thermal losses (Q_{loss}) can be found through Equation (2.5).

3.4.7 Efficiency

By knowing the useful energy, solar radiation, and the concentrated area, efficiency can be found from Equation (2.20).

4. RESULTS AND DISCUSSION

4.1 Introduction

This chapter provides a detailed description of the numerous experimental outcomes obtained during the testing phases. Solar radiation is an essential factor in the applications of solar energy. Solar radiation is expected to increase when transitioning from Spring to Summer due to the Earth's position around the Sun throughout the annular cycle. April and May were the periods of the experiential study as these Months represent the transition between Spring and Summer; where in Section 4.3, the intensity of solar radiation was studied over four days in April and four days in May to understand the change in solar radiation. The reasons for taking the reading on different days in each of these two Months include: a) the start of the experimental tests for each Month is ideal to be on an uncloudy day, b) during the heating process, the water inside the tank retains temperature for a while; therefore, the test reading for the consequence days was taking on the third day after previous test day (i.e., for May, the test start on the 6th, then the next test day was on the 9^{th} to allow enough time for the water in the system to cool down). The experimental tests results over four days in May were used throughout Sections 4.4 to 4.12 to study 1) the relationship between solar radiation and in-and-out water temperature, 2) the flow rate and temperature of the water exiting the receiver, 3) the effect of wind speed on the receiver's heat loss, 4) relationship between the receiver's heat loss and the receiver's temperature, 5) effect of flow rate on the thermal loss of solar collector, 6) relationship between solar radiation and optical energy, 7) relationship between solar radiation and useful energy, 8) effect of flow rate on overall efficiency, and 9) the relationship between overall efficiency and operating conditions. These experiments are conducted in Iraq Erbil – Kasnazanat at 44.12 degrees longitude and 36.21 degrees latitude, where the system starts operating from 9:00 AM until 6:00 PM.

4.2 System Engineering Characteristics

The parabolic solar concentrator system is an effective system that converts solar energy into thermal energy, where the solar rays that fall are concentrated in the focus using reflective material such as glass - aluminium - mylar sheets. Table 4.1 shows the calculation of the system engineering characteristics via the excel program (Ahmed *et al.* 2020). The calculations are as shown in Appendix 2.

Table 4.1 Engineering characteristics of the concentrator

Engineering Characteristics	**Value**
Parabola aperture diameter (d)	1.4 m
concentrator aperture area	1.5386 m^2
The area of the solar concentrator	1.599 m^2
parabola depth (h)	0.14 m
Total space of the receiver	0.12791 m^2
focal length (f)	0.875 m
Rim angle Ψ	43.6°
f/d	0.625

4.3 Change in Solar Radiation Intensity with Time for April and May

Solar radiation is considered an important factor in solar energy applications because solar concentrators depend on the intensity of solar radiation. The intensity of solar radiation and brightness varies from day to day due to the Earth's position around the Sun throughout the annular cycle. This is affected by several factors such as (geo-location, air mass flu, clouds, wind) and other factors that have an impact on the efficiency of the system, as shown in Table 4.2 and Figure 4.1 which show the change in the intensity of solar radiation on the concentrating with time during the months of April and May. The results are in agreement with Rafeeu and Ab'Kadir (2012) and Newton (2007).

Table 4.2 The relation between solar radiation with time for the months of April and May

Day	7th of April	11th of April	16th of April	22nd of April	6th of May	9th of May	12th of May	16th May
Time	Solar Radiation (W/m^2)							
9:00 AM	440	450	450	460	480	490	500	500
10:00 AM	530	550	560	570	590	600	610	620
11:00 AM	620	650	680	700	730	720	740	750
12:00 PM	740	770	800	810	840	850	860	870
1:00 PM	500	820	850	870	900	910	930	940
2:00 PM	530	760	800	820	860	870	880	890
3:00 PM	600	690	700	710	760	770	790	800
4:00 PM	360	560	590	590	630	650	680	690
5:00 PM	300	320	380	400	450	460	480	500
6:00 PM	50	80	90	100	130	150	170	200

Figure 4.1 A shows the relationship between the intensity of solar radiation and time at the beginning and end of April. It is noticed that on 7th of April 2022 the intensity of solar radiation was 440 W/m^2 at 9:00 AM and began rising gradually until reaching its highest value at twelve o'clock in the afternoon in which the intensity of solar radiation reached 740 W/m^2. After that, it began to decrease as a result of the decrease in the intensity of solar radiation due to the appearance of clouds at one o'clock in the afternoon. Then, it began to increase at three o'clock in the afternoon, and finally began gradually decreasing until six o'clock in the evening. However, on 22nd of April the intensity of solar radiation was 460 W/m^2 at nine o'clock in the morning and began to rise until it reached its highest value at one o'clock in the afternoon reaching 870 W/m^2, and finally began to decrease gradually until six o'clock in the evening. The results are in agreement with Rafeeu and Ab'Kadir (2012).

Figure 4.1 B shows the change in the intensity of solar radiation at the beginning and middle of the month of May. It is noticed that the solar radiation at the beginning of May on 6th of May started from 480 W/m^2 at the beginning of the test time at nine o'clock in the morning, then it began to increase gradually with the progression of time until one in the afternoon reaching 900 W/m^2. Finally, it gradually began to decrease until it reached 130 W/m^2 at the end of the test time at six o'clock in the evening. As for the middle of May the 16th, it is also noticed that the intensity of solar radiation is higher than its value at the beginning of the month. It is clear from Figure 4.1 B that the solar radiation started from 500 W/m^2 at nine o’clock in the morning until it reached one o’clock in the afternoon with 940 W/m^2. Finally, it gradually began to decrease until it reached 200 W/m^2 at the end of the test time at six o'clock in the evening.

Figure 4.1 C shows the relation between the intensity of solar radiation and time for two different days of the months of April and May. It is noted that the solar radiation on 11th of April at nine o’clock in the morning was 450 W/m^2 and began to rise gradually until one o'clock in the afternoon reaching 820 W/m^2. It began to gradually decline as a result of the decrease in solar radiation, which is due to the change in the movement of the sun's path towards sunset. As for the 9th of May, the solar radiation began high and since the early hours of the morning, it reached 490 W/m^2 until reaching its highest value at one o'clock in the afternoon with 910 W/m^2. It gradually decreased as it reached 150 W/m^2 at the end of the test time at six o'clock in the evening. The results are in agreement with Starakis and Halkia (2010) and Alrofiae and Kadhem (2012).

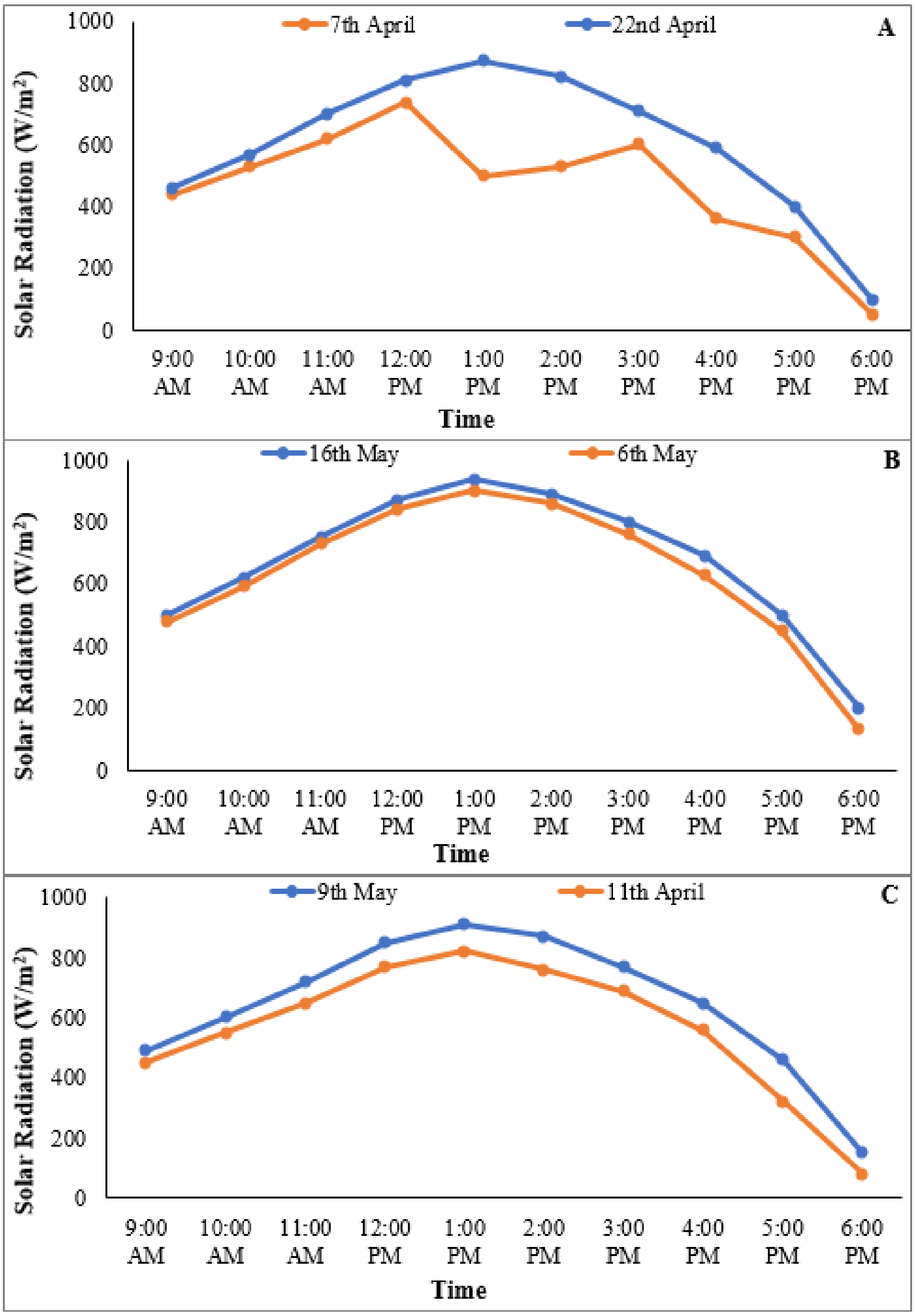

Figure 4.1 The intensity of solar radiation and time during selected days in April and May

4.4 Change in Solar Radiation Intensity and Water Temperature for May

Table 4.3 and Figure 4.2 show the effect of the change in the solar radiation intensity on each water temperature entering and exiting the receiver over time.

Table 4.3 Temperature of the water entering and leaving the receiver for May

Time	T_{in} (K)	T_{out} (K)	T_{in} (K)	T_{out} (K)	T_{in} (K)	T_{out} (K)	T_{in} (K)	T_{out} (K)
	6th of May		9th of May		12th of May		16th of May	
	Mass flow rate 0.0055 (kg/s)		Mass flow rate 0.009 (kg/s)		Mass flow rate 0.022 (kg/s)		Mass flow rate 0.028 (kg/s)	
9:00 AM	304	318	305	313	306	310	306	309
10:00 AM	312	343	311	328	310	318	308	315
11:00 AM	322	371	318	347	316	326	312	322
12:00 PM	333	393	330	363	323	335	317	330
1:00 PM	347	408	342	377	331	342	324	335
2:00 PM	359	413	351	385	338	344	328	338
3:00 PM	364	407	357	382	339	343	329	337
4:00 PM	363	393	356	376	337	340	327	336
5:00 PM	359	380	353	368	333	336	325	333
6:00 PM	350	366	348	357	329	331	322	328

Figure 4.2 A show the effect of the change in the intensity of solar radiation on each of the water temperature entering and exiting the receiver over time during the 6th of May at a mass flow rate of 0.0055 kg/s. It is noted from the table that the intensity of solar radiation at nine o'clock in the morning reached 480 W/m^2 and gradually began to rise until it reached its highest value at one o'clock in the afternoon with 900 W/m^2. It begins to decrease gradually until reaching 130 W/m^2 at 6:00 PM. The temperature of the water entering the receiver was 304 K at nine o'clock in the morning and begins to gradually increase until it is reaching 364 K at three o'clock in the afternoon, then it begins to gradually decrease at the end of the test time. The water temperature coming out of the receiver reaches 318 K at nine o'clock in the morning. Its highest value is at two o'clock in the afternoon reaching 413 K when the ambient temperature of the work area is 309 K. The results agree with Sakhare and Kapatkar (2014).

Figure 4.2 B shows the change in the amount of solar radiation and its effect on the temperature of the water entering and exiting the receiver on May 9th at a mass flow rate of 0.009 kg/s. The intensity of solar radiation at nine o'clock in the morning is 490 W/m^2 and begins to gradually increase over time until it reaches 910 W/m^2 at one o'clock in the afternoon. As for the temperature of the water entering the receiver, it is 305 K at nine o’clock in the morning. It continued to rise with the progression of time and the increase in solar radiation until reaching 357 K at three o’clock in the afternoon. As for the water exiting the receiver, it is noted that it begins with 313 K at nine o’clock in the morning to 385 K at two o’clock in the afternoon. It begins to decrease as a result of the decrease in the intensity of solar radiation with the passage of time until it reaches 357 K at six o’clock p.m. The increase in solar radiation works to raise the temperature of the receiver as it behaves like a black body as a result of the increase in solar radiation, which in turn raises the temperature of the receiver. According to Stephen Boltzmann's law (E = σT4), when the receiver temperature rises, the heat is transmitted by conduction to the water, whose temperature also rises.

Figure 4.2 C shows the change in the amount of solar radiation and its effect on the temperature of the water entering and exiting the receiver on May 12^{th} at a mass flow rate of 0.022 kg/s. The intensity of solar radiation at nine o'clock in the morning is 500 W/m^2 and begins to gradually increase over time until it reaches 930 W/m^2 at one o'clock in the afternoon. As for the temperature of the water entering the receiver, it is 306 K at nine o’clock in the morning. It continued to rise with the progression of time and the increase in solar radiation until reaching 339 K at three o’clock in the afternoon. As for the water exiting the receiver, it is noted that it begins with 310 K at nine o’clock in the morning to 344 K at two o’clock in the afternoon (when the ambient temperature is 310 K). It begins to decrease as a result of the decrease in the intensity of solar radiation with the passage of time until it reaches 331 K at 6:00 PM.

Figure 4.2 D shows the change in the amount of solar radiation and its effect on the temperature of the water entering and exiting the receiver on May 16^{th} at a mass flow rate of 0.028 kg/s. The intensity of solar radiation at nine o'clock in the morning is 500 W/m^2 and begins to gradually increase over time until it reaches the highest value with 940 W/m^2 at one o'clock in the afternoon. As for the temperature of the water entering the receiver, it 306 K at nine o’clock in the morning. It continues to rise with the progression of time and the increase in solar radiation until reaching 329 K at three o’clock in the afternoon (when the ambient temperature is 311 K). As for the water exiting the receiver, it is noted that it begins with 309 K at nine o’clock in the morning to 338 K at two o’clock in the afternoon. It begins to decrease as a result of the decrease in the intensity of solar radiation with the passage of time until it reaches 328 K at 6:00 PM. The results are in agreement with Tadros *et al.* (2014).

It is clear that the temperature of the water exiting the receiver through the speed of the water flow from the beginning to end slowly declines even after the decrease in the intensity of solar radiation. This is due to the receiver's retention of heat as a result of its isolation by a thermal insulator (thermal wool), until the solar radiation decreases greatly. The ambient air temperature decreases, then the temperature of the water exiting the receiver decreases because the heating process inside the receiver has become low. The results are in agreement with Newton (2007). The calculations are as shown in Appendix 2.

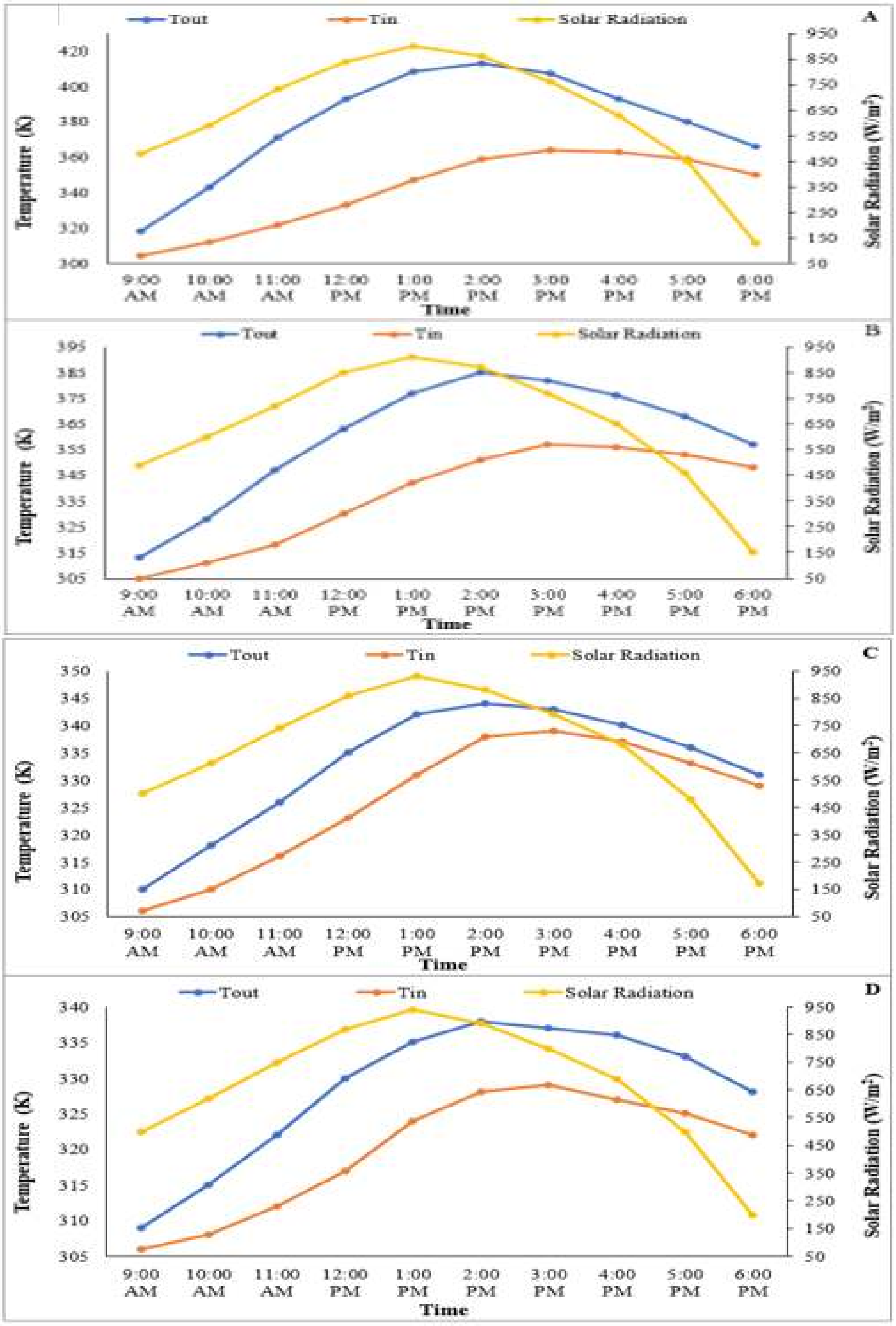

Figure 4.2 Solar radiation and water temperature on May 6th (A), May 9th (B), May 12th (C), and May 16th (D)

4.5 Effect of Mass Flow Rate on Temperature of Water Existing the Receiver for May

The mass flow rate has a significant effect on the temperature of the water exiting the receiver. The highest temperature of the water exiting the receiver in May was at a mass flow rate of 0.0055 kg/s and its highest value was 413 K at two o'clock in the afternoon, and the lowest at a mass flow rate of 0.009 kg/s at the same time reaching 385 K at two o'clock in the afternoon. The flow rate of 0.022 kg/s was lower than the previous one, as the temperature reached 344 K. As a result of the flow of 0.028 kg/s, the water exit temperature from the receiver was 338 K at two o'clock in the afternoon. The highest temperature of the water exiting the receiver is at a mass flow rate of 0.0055 kg/s, as shown in Table 4.4 and Figure 4.3. The reason for this is that the lower the mass flow rate of the working fluid (water), the longer its stay inside the receiver, which increases the period of heat transfer by conduction and thus increases the temperature of the water exiting the receiver. The results are in agreement with Zedan *et al.* (2017) and García and Valladares (2009).

Table 4.4 Outlet water temperature from receiver for the four selected days of May

Time	T_{out} (K) 6th of May, Mass flow rate 0.0055 kg/s	T_{out} (K) 9th of May, Mass flow rate 0.009 kg/s	T_{out} (K) 12th of May, Mass flow rate 0.022 kg/s	T_{out} (K) 16th of May, Mass flow rate 0.028 kg/s
9:00 AM	318	313	310	309
10:00 AM	343	328	318	315
11:00 AM	371	347	326	322
12:00 PM	393	363	335	330
1:00 PM	408	377	342	335
2:00 PM	413	385	344	338
3:00 PM	407	382	343	337
4:00 PM	393	376	340	336
5:00 PM	380	368	336	333
6:00 PM	366	357	331	328

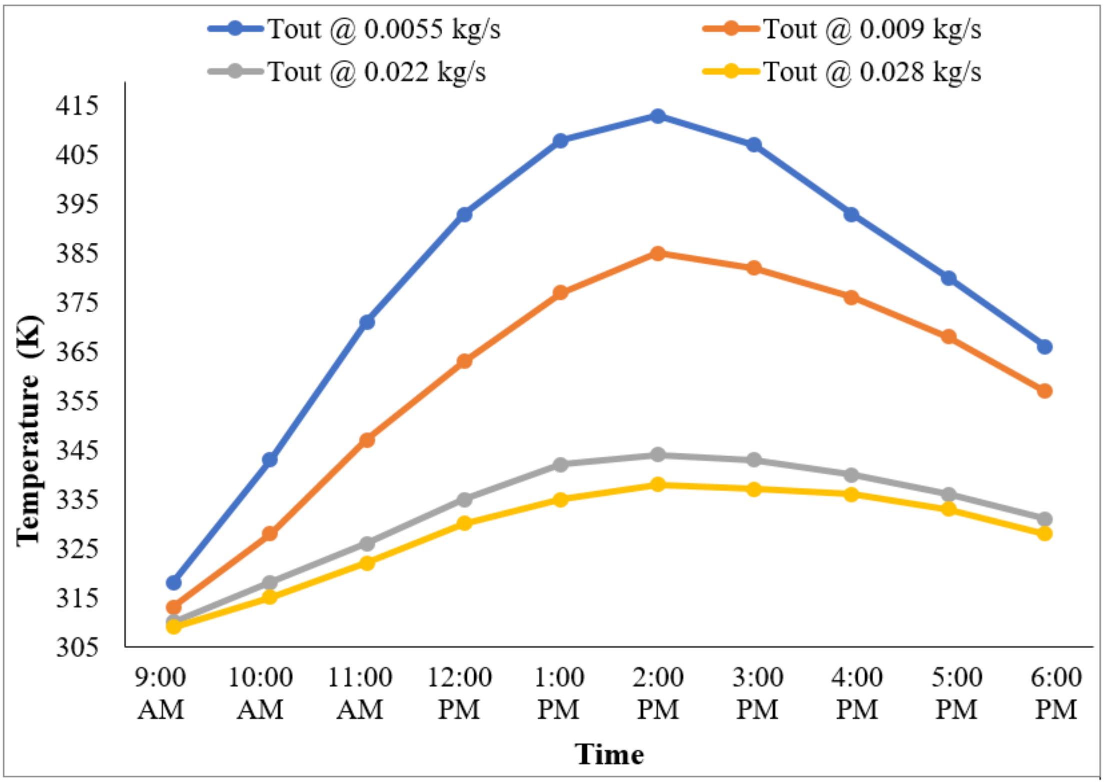

Figure 4.3 The effect of the change in the mass flow rate on the temperature of the water exiting the receiver for the selected four days of May

4.6 Effect of Wind Speed on Heat Loss of the Receiver

There are many reasons for thermal losses, including the decrease in the amount of solar radiation, which may be due to the passage of a number of clouds, the influence of winds, or other weather factors. They are the losses resulting from thermal load, in which the receiver loses a quantity of (Q_{loss}) it's thermal energy as shown in Table 4.5 and Figure 4.4. that the heat losses for the month of May on the 6^{th} day were 100.55 W at a wind speed of 0.45 m/s, the mass flow rate was 0.0055 kg/s, and less of which at a wind speed of 0.475 m/s. The heat losses on the 9^{th} day of May was 80.77 W at a mass flow rate was 0.009 kg/s, while at a flow rate of 0.022 kg/s, the coefficient of heat losses (Q_{loss}) was 52.49 W for the 12^{th} day of May at a wind speed 0.85 m/s. The heat loss coefficient (Q_{loss}) on the 16^{th} day of May was 30.97 W at a wind speed of 0.55 m/s and flow rate of 0.028 kg/s. Figure 4.4 show the relationship between heat loss with wind speed. This increase explains Stephen Boltzmann's law, where the radiation emitted from a hot source is proportional to the fourth power of the source temperature. The effect of the ambient temperature is represented by the regression in the heat loss coefficient via the radiation of the receiver at any given temperature. Thus, the receiver components and pipes must be isolated from the surroundings to reduce losses. The results are in agreement with Duffie and Beckman (1980).

Table 4.5 Wind speed and corresponding receiver's heat loss for the four selected days of May

Time	Wind Speed (m/s)	Heat Loss (W)	Wind Speed (m/s)	Heat Loss (W)	Wind Speed (m/s)	Heat Loss (W)	Wind Speed (m/s)	Heat Loss (W)
	6th of May		9th of May		12th of May		16th of May	
9:00 AM	0.2	6.96	0.15	3.67	0.5	2.66	0.325	1.75
10:00 AM	0.225	23.28	0.25	14.49	0.55	9.73	0.35	5.22
11:00 AM	0.3	46.05	0.275	28.30	0.6	18.81	0.375	10.18
12:00 PM	0.35	64.98	0.3	44.09	0.65	28.61	0.4	16.66
1:00 PM	0.4	85.22	0.35	58.05	0.7	39.75	0.45	24.0
2:00 PM	0.425	97.03	0.45	76.06	0.75	46.70	0.5	28.51
3:00 PM	0.45	100.55	0.475	80.77	0.85	52.49	0.55	30.97
4:00 PM	0.425	89.84	0.45	76.60	0.9	51.13	0.5	30.27
5:00 PM	0.4	78.30	0.425	69.02	0.85	46.22	0.45	28.18
6:00 PM	0.375	64.65	0.4	58.68	0.8	40.69	0.4	24.28

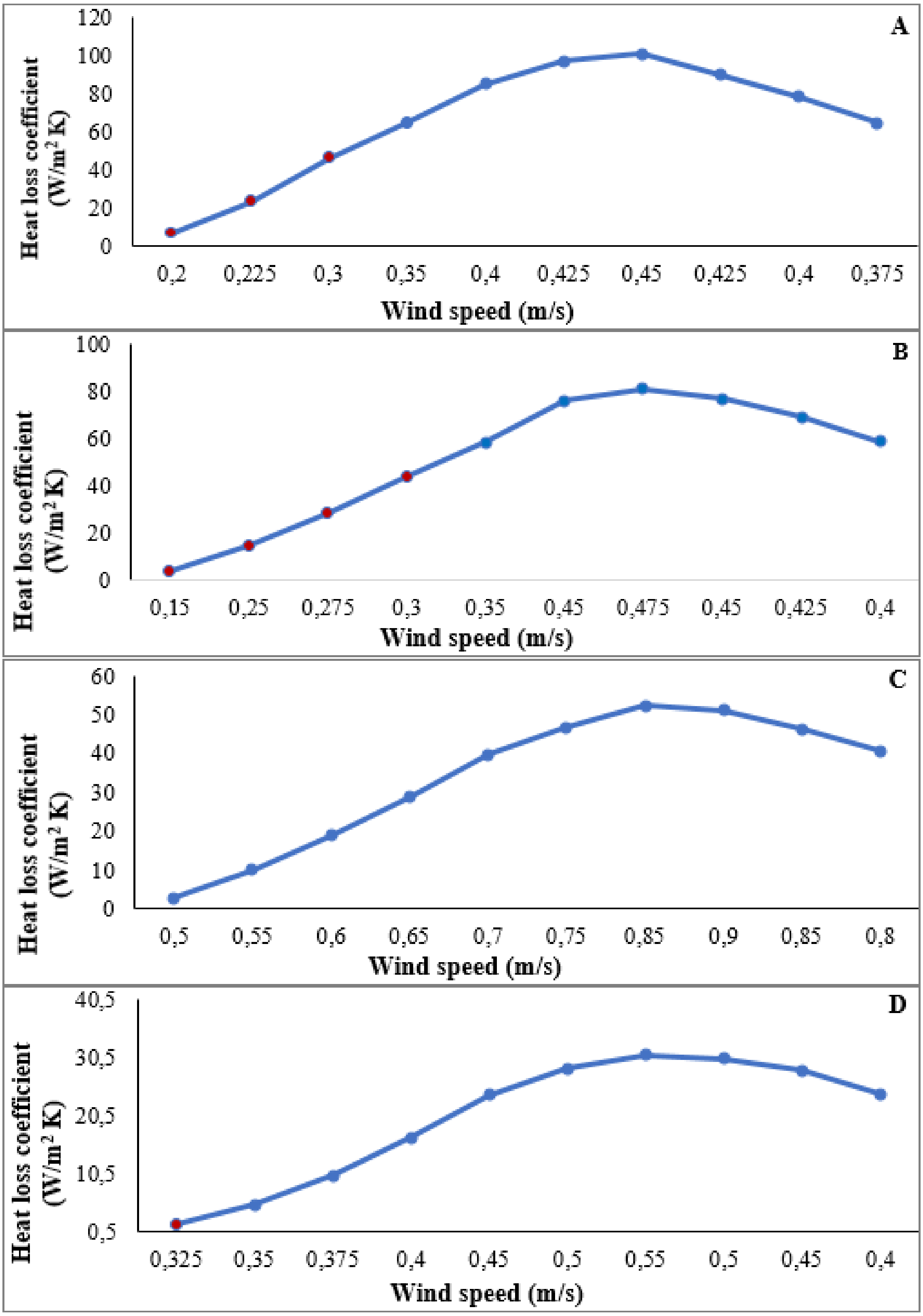

Figure 4.4 The effect of wind speed on receivers' heat loss on May 6th (A), May 9th (B), May 12th (C), and May 16th (D)

4.7 Relationship Between the Receiver's Heat Loss and Average Temperature

The thermal losses are increased with the increasing of receiver temperature as shown in Table 4.6 and Figure 4.5 which shows the trend of heat loss (Q_{loss}) from the receiver by the average outlet temperature at a constant flow. The losses resulting from thermal convection lost by the receiver contain a quantity of its thermal energy. As shown in Figure 4.5, the highest thermal losses (Q_{loss}) of 100.55 W have been recorded on the 6th of May at the average temperature of the receiver was 385.5 K, While the heat loss on 9th May dropped to 80.7 W at the average temperature of the receiver 369.5 K. On the 12th of May, the heat losses were 52.4 W, and the receiver temperature was 341 K. The heat losses were 30.9 W on the 16th of May at the average temperature of the receiver 333 K. the reason of this behaviour is due to the thermal losses are directly proportional to the increase in the average temperature of the receiver and the coefficient of thermal losses so that the higher the temperature of the receiver, the greater the thermal losses. The results are in agreement with Mancini (2015) and Bissert *et al.* (2016).

Table 4.6 The relation between heat loss and the average receiver temperature

Time	**T Receiver (K)**	**Heat Loss (W)**	**T Receiver (K)**	**Heat Loss (W)**	**T Receiver (K)**	**Heat Loss (W)**	**T Receiver (K)**	**Heat Loss (W)**
	6th of May		9th of May		12th of May		16th of May	
9:00 AM	311	6.96	309	3.67	308	2.66	307.5	1.75
10:00 AM	327.5	23.28	319.5	14.49	314	9.73	311.5	5.22
11:00 AM	346.5	46.05	332.5	28.30	321	18.81	317	10.18
12:00 PM	363	64.98	346.5	44.09	329	28.61	323.5	16.66
1:00 PM	377.5	85.22	359.5	58.05	336.5	39.75	329.5	24.0
2:00 PM	386	97.03	368	76.06	341	46.70	333	28.51
3:00 PM	385.5	100.55	369.5	80.77	341	52.49	333	30.97
4:00 PM	378	89.84	366	76.60	338.5	51.13	331.5	30.27
5:00 PM	369.5	78.30	360.5	69.02	334.5	46.22	329	28.18
6:00 PM	358	64.65	352.5	58.68	330	40.69	325	24.28

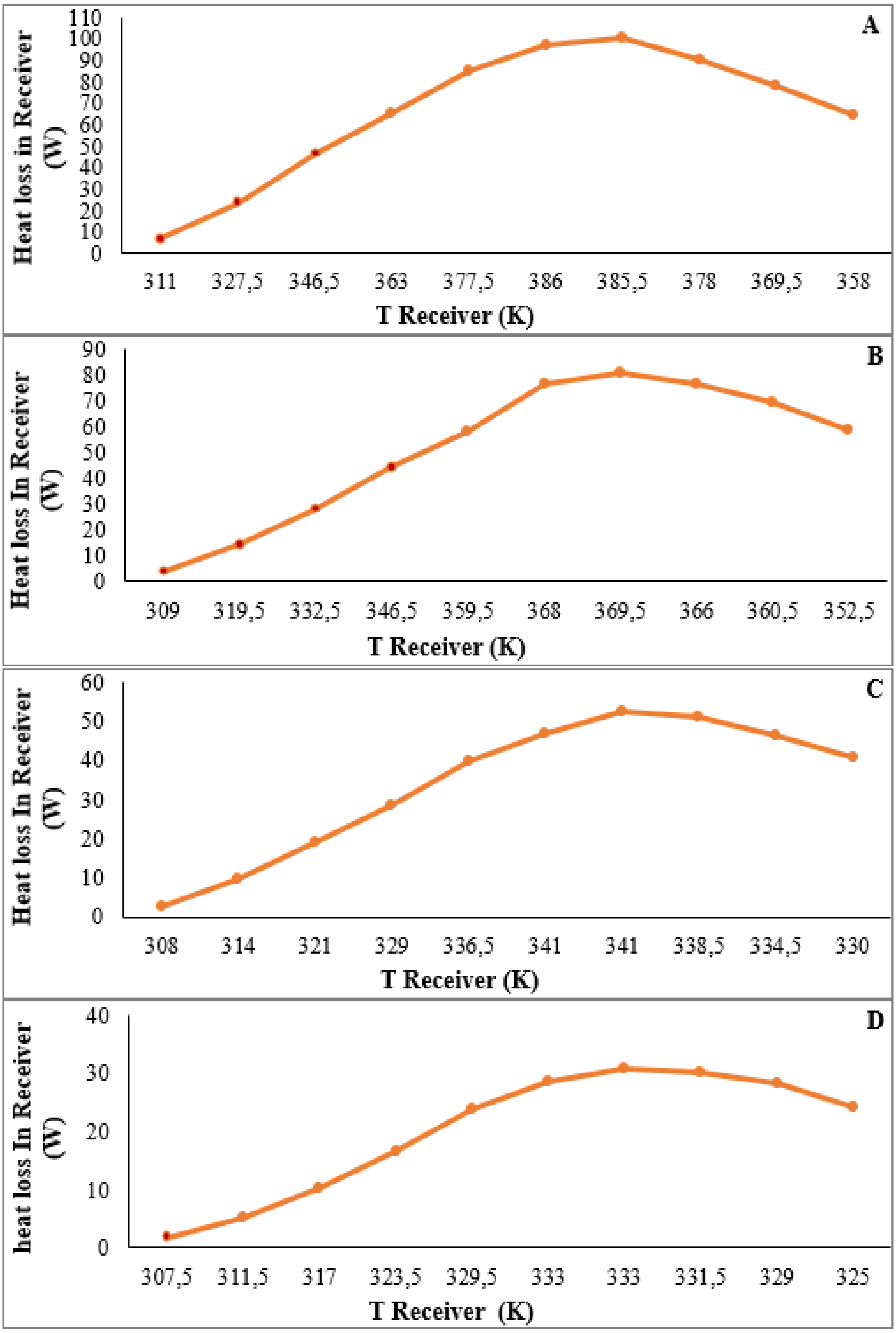

Figure 4.5 The relation between heat loss and the average receiver temperature on May 6th (A), May 9th (B), May 12th (C), and May 16th (D)

4.8 Effect of Mass Flow Rate on Thermal Losses of the Solar Collector

There are many reasons for the thermal losses of the dish solar collector, including the decrease in the amount of solar radiation, which may be due to the passage of a number of clouds, the influence of winds or other weather factors. Another reason is the losses resulting from thermal convection in which the receiver loses a quantity of its thermal energy. As shown in Figure 4.6, the thermal losses for the month of May are highest at a mass flow rate 0.0055 kg/s and lowest at a flow rate 0.009 kg/s. Thus, the flow rate 0.022 kg/s and the mass flow rate 0.028 kg/s are lower, respectively. The reason for this is that the thermal losses are directly proportional to the increase in the temperature of the water exiting the receiver and the thermal losses coefficient (Q_{loss}), The results are in agreement with Mancini (2015).

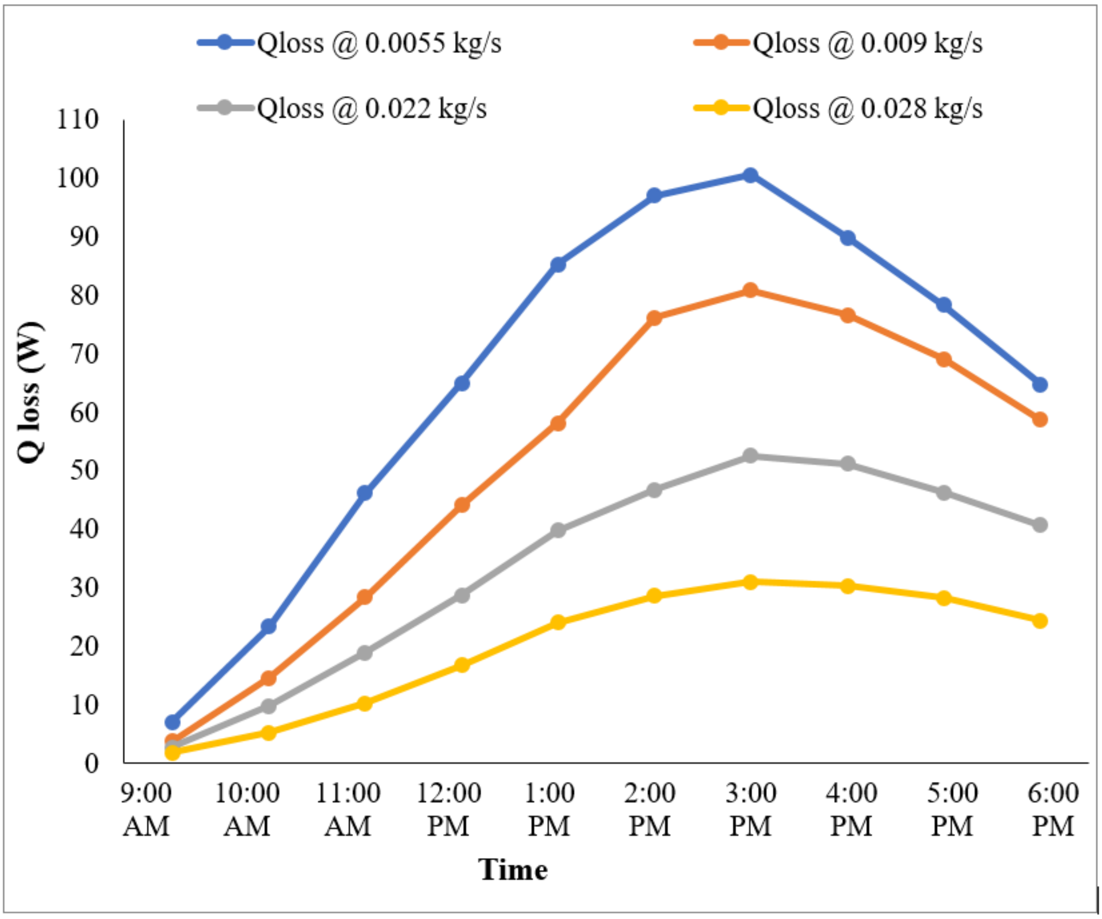

Figure 4.6 Effect of mass flow rate on the solar dish collector

4.9 Relationship Between Solar Radiation and Optical Energy of the Solar Dish Collector

The intensity of solar radiation is directly proportional to the optical energy, as the greater the intensity of solar radiation, the greater the optical energy with the passage of time in a day, as shown in Table 4.7 and Figure 4.7 which shows the relation between intensity with time and optical energy for the 6th,9th, 12th, and 16th of May 2022. It is noticed that the optical energy increases with the increase of time, and this is due to the optical energy increase resulting from the conversion of solar radiation in short and long wavelengths into heat. This is due to the effectiveness of the concentrator in concentrating the radiation as well as the effectiveness of the receiver in retaining heat for the longest possible period, to benefit from the processes of heating the heat carrier medium. The dish collector depends on several factors, including radiation, the type of reflector used, the size of the collector, and the type of receiver. The relationship between solar radiation and optical energy is direct, the higher the radiation, the higher the optical energy, as shown in Figure 4.7. The results are in agreement with Sulaiman *et al.* (2012) and Alrofiae and Kadhem (2012).

Table 4.7 The relation between solar radiation (I_a) and optical energy (Q_{opt}) for the four selected days of May

Time	I_a (W/m^2)	Q_{opt} (W)	I_a (W/m^2)	Q_{opt} (W)	I_a (W/m^2)	Q_{opt} (W)	I_a (W/m^2)	Q_{opt} (W)
	6th of May		9th of May		12th of May		16th of May	
9:00 AM	480	666.5	490	680.4	500	694.3	500	694.3
10:00 AM	590	819.3	600	833.2	610	847.0	620	860.9
11:00 AM	730	1013.7	720	999.8	740	1027.5	750	1041.4
12:00 PM	840	1166.4	850	1180.3	860	1194.2	870	1208.1
1:00 PM	900	1249.7	910	1263.6	930	1291.4	940	1305.1
2:00 PM	860	1194.2	870	1208.1	880	1221.9	890	1235.8
3:00 PM	760	1055.3	770	1069.2	790	1096.9	800	1110.9
4:00 PM	630	874.8	650	902.6	680	944.2	690	958.1
5:00 PM	450	624.9	460	638.7	480	666.5	500	694.3
6:00 PM	130	180.5	150	208.3	170	236.1	200	277.7

Figure 4.7 A shows the relationship between the intensity of solar radiation with time and optical energy. It was noted at the beginning of May on day Six that the intensity of solar

radiation was 480 W/m^2 at nine o'clock in the morning and Q_{opt} was 666.52 W. It began gradually ascending until one o'clock in the afternoon where the intensity of solar radiation reached 900 W/m^2 and Q_{opt} 1249.73 W. It then began to gradually decrease until it reached the end of the test at six o'clock in the evening. Figure 4.7 B shows the relationship between the intensity of solar radiation and Q_{opt} for the 9th of May. It is noticed at the beginning of the test at nine o'clock in the morning that the intensity of solar radiation was 490 W/m^2 and Q_{opt} 680.41 W. It gradually began to rise at one o'clock noon at the highest radiation on a clear day with 910 W/m^2, where the Q_{opt} was 1263.61 W. Figure 4.7 C shows the relation between the intensity of solar radiation and Q-optical with time on the day 12th of May. It is noticed at the beginning of the test at nine o'clock in the morning that the radiation was 500 W/m^2 and Q_{opt} 694.29 W. However, at one o'clock in the afternoon and at the highest radiation 930 W/m^2, the Q_{opt} was 1291.39 W. Figure 4.7 D the relationship is shown between radiation and Q_{opt} with time on the 16th of May. At the beginning of the test at nine o'clock in the morning, the radiation intensity was 500 W/m^2 and Q_{opt} 694.29 W. It began to gradually rise until it reached one o'clock in the afternoon with the intensity of solar radiation 940 W/m^2 and Q_{opt} 1305.27 W. After that, it began to gradually decrease until it reached the end of the test at six o'clock in the evening when the intensity of solar radiation was 200 W/m^2 and Q_{opt} 277.72 W. This agrees with García and Velázquez (2009). The calculations are in Appendix 2.

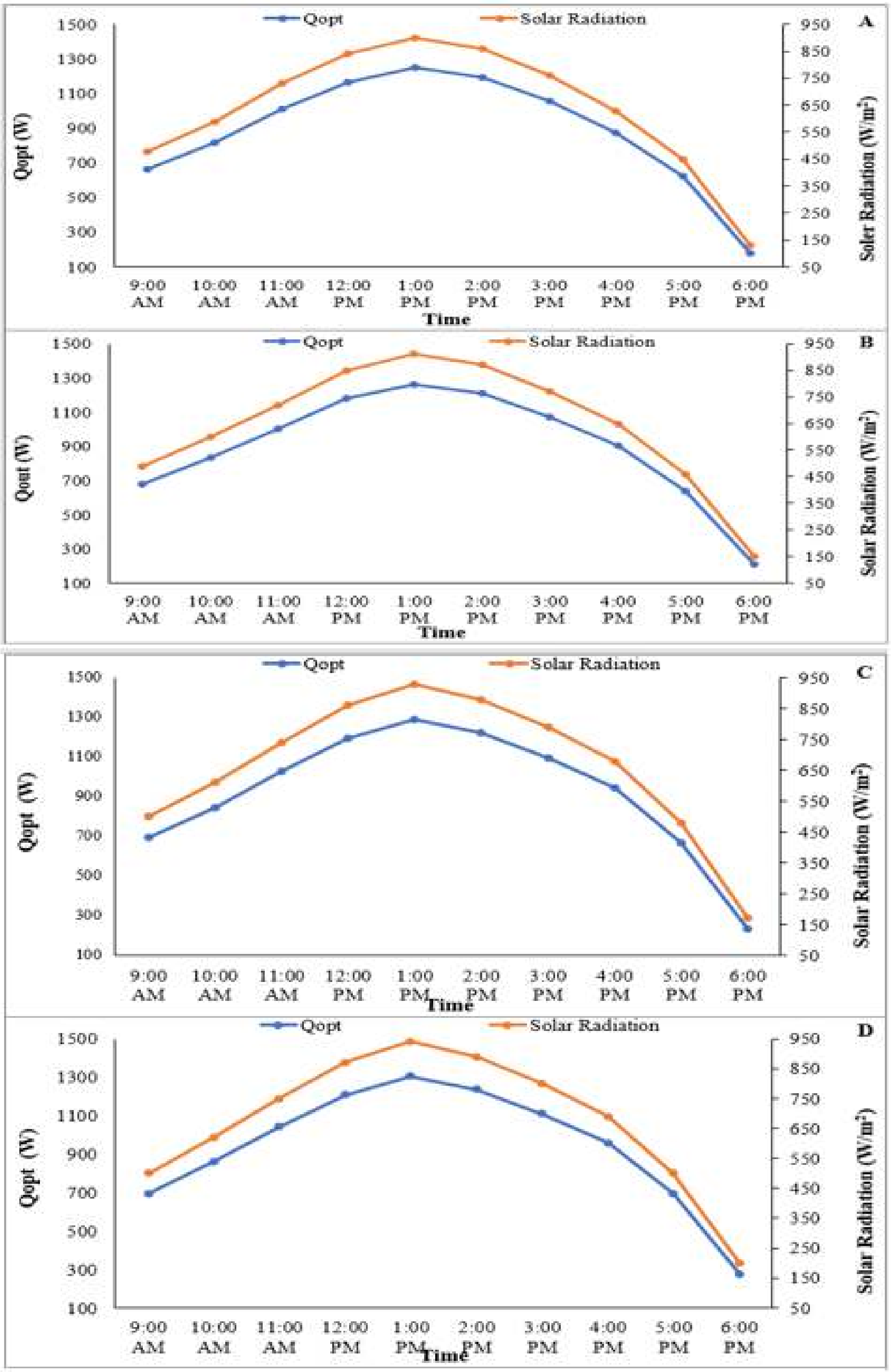

Figure 4.7 The relationship between solar radiation and optical energy on May 6th (A), May 9th (B), May 12th (C), and May 16th (D)

4.10 Relationship Between Solar Radiation and Useful Energy Profit (Q out) of the Solar Dish Collector

The intensity of solar radiation is directly proportional to the profit of useful energy, as the greater the intensity of solar radiation, the greater the profit of useful energy with the passage of time, as shown in Figure 4.8. It is noted from Figure 4.8 that the profit of useful energy increases with the increase of time, and this is due to the Q-optical increase resulting from the conversion of solar radiation in short and long wavelengths into heat. This is a result of the efficiency of the concentrator in concentrating solar radiation as well as the effectiveness of the receiver in retaining heat for the longest possible period to be benefited from in the heating processes of the heat carrier medium (water). The results are in agreement with Alrofiae and Kadhem (2012).

Figure 4.8 A shows that the profit of the useful energy at a mass flow rate of 0.0055 kg/s is 1164 W at a solar radiation intensity of 900 W/m^2. Figure 4.8 B shows that the useful energy profit is 1205 W at a mass flow rate of 0.009 kg/s and a solar radiation intensity of 910 W/m^2. Figure 4.8 C shows that the highest value reached for the useful energy profit useful Energy is 1251 W at a mass flow rate of 0.022 kg/s and the intensity of solar radiation is 930 W/m^2 at 1 pm. Figure 4.8 D shows that the highest useful energy is obtained 1281 W at a mass flow rate of 0.028 kg/s and a radiation intensity of 940 W/m^2 at 1 pm. It is noticed from Figure 4.8 A, B, C, and D that the highest useful energy gain is obtained at a mass flow rate of 0.028 kg/s, and the lowest useful energy is at a flow rate of 0.0055 kg/s. This is attributed to the increasing amount of solar radiation falling on the concentrator in the beginning and middle of May and on thermal losses and flow rate of the working fluid (water). The results are in agreement with Sagade (2015) and Hafez *et al.* (2018).

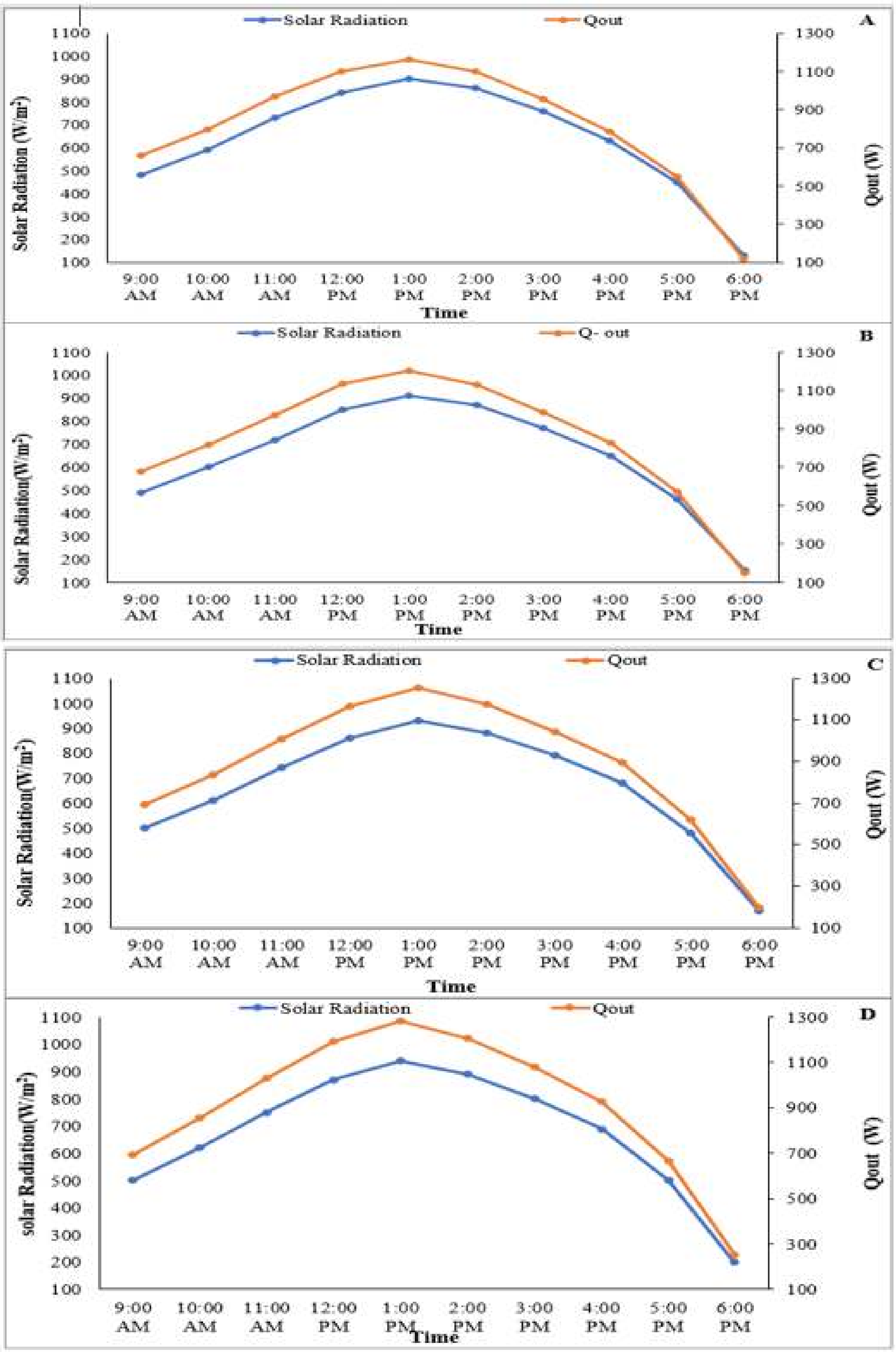

Figure 4.8 The relationship between solar radiation and useful energy on May 6th (A), May 9th (B), May 12th (C), and May 16th (D)

4.11 Effect of Mass Flow Rate on Overall Efficiency of the Solar Dish Collector

The overall efficiency of the solar dish collector is affected by the optical losses associated with the materials used to manufacture the solar dish collector, the operating conditions, the focus of the receiver, the aperture of the receiver, the area of the solar concentrator, and other factors that lead to the efficiency of the solar collector. Figure 4.9 shows the total efficiency of the solar collector at mass flow rates 0.0055 kg/s, 0.009 kg/s, 0.022 kg/s, and 0.028 kg/s for the month of May. The figure shows that the efficiency during the month of May increases with an increase in the mass flow rate and decreases with a decrease of it. The highest efficiency was at a mass flow rate of 0.028 kg/s and less than that at a mass flow rate of 0.022 kg/s, and so on, respectively for the flow rate of 0.009 kg/s and the flow rate of 0.0055 kg/s. It is noted from the figure that the highest process efficiency was at a mass flow rate of 0.028 kg/s. This is due to the fact that the efficiency is directly proportional to the energy acquired for the collector, which in turn depends on the mass flow rate, which increases as it increases and decreases as it decreases. The results are in agreement with Sagade (2015).

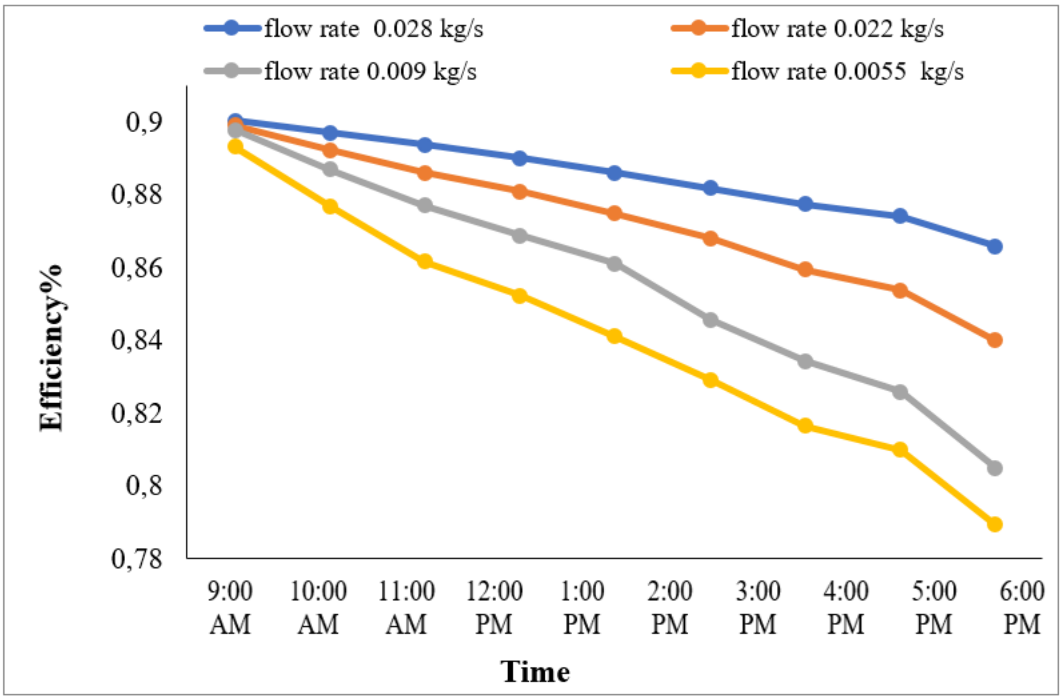

Figure 4.9 Effect of mass flow rate on overall efficiency of the solar dish collector for the four selected days of May

4.12 Relationship Between the Solar Dish Collector Overall Efficiency and Operating Conditions

According to the heat transfer process, the efficiency of the thermal system is affected by both thermal losses and optical losses. The amount of these losses depends on the design of the system and the operating conditions. The losses of optical energy result from the reflectivity of the concentrator, the absorbance of the receiver as well as the area and amount of benefit from the radiation reaching the concentrator. Moreover, there is the receiving material in the operating conditions and the fact that there is a loss in useful energy. The results are in agreement with Folaranmi (2009) and Naveenkumar *et al.* (2021).

These losses occur, especially in the receiver, and in the tank and connection pipes, by convection and radiation. The amount of these losses depends on the type of receiver, the geometrical form, the aperture area, the type of reflector, the type of tank insulation, and the connection pipes. The factors mentioned above contribute to the efficiency of the thermal system. The results are in agreement with Duffie and Beckman (2013). In addition, the operating temperature increases the heat loss coefficient. The longer the operating time, the greater the losses, as shown in Figure 4.10, because the air temperature is inversely proportional to the receiver temperature. As it decreases with an increase in the temperature of the receiver, so does heat loss, which results in thermal equilibrium between the receiver metal and its surroundings. Accordingly, the components are permanently isolated from the environment to reduce losses, as the insulation increases the thermal energy, which is of great benefit, and thus increases the efficiency of the heater. Figure 4.10 shows the variance of instantaneous efficiency with the operating temperature (T_{in} - T_{air}) of the receiver. The system's efficiency decreases with the receiver's temperature since the radiated lost energy is directly proportional to the fourth temperature exponent according to Stefan Bolt-Zmann's law (E= σ T4). The results are in agreement with Kumar *et al.* (2015).

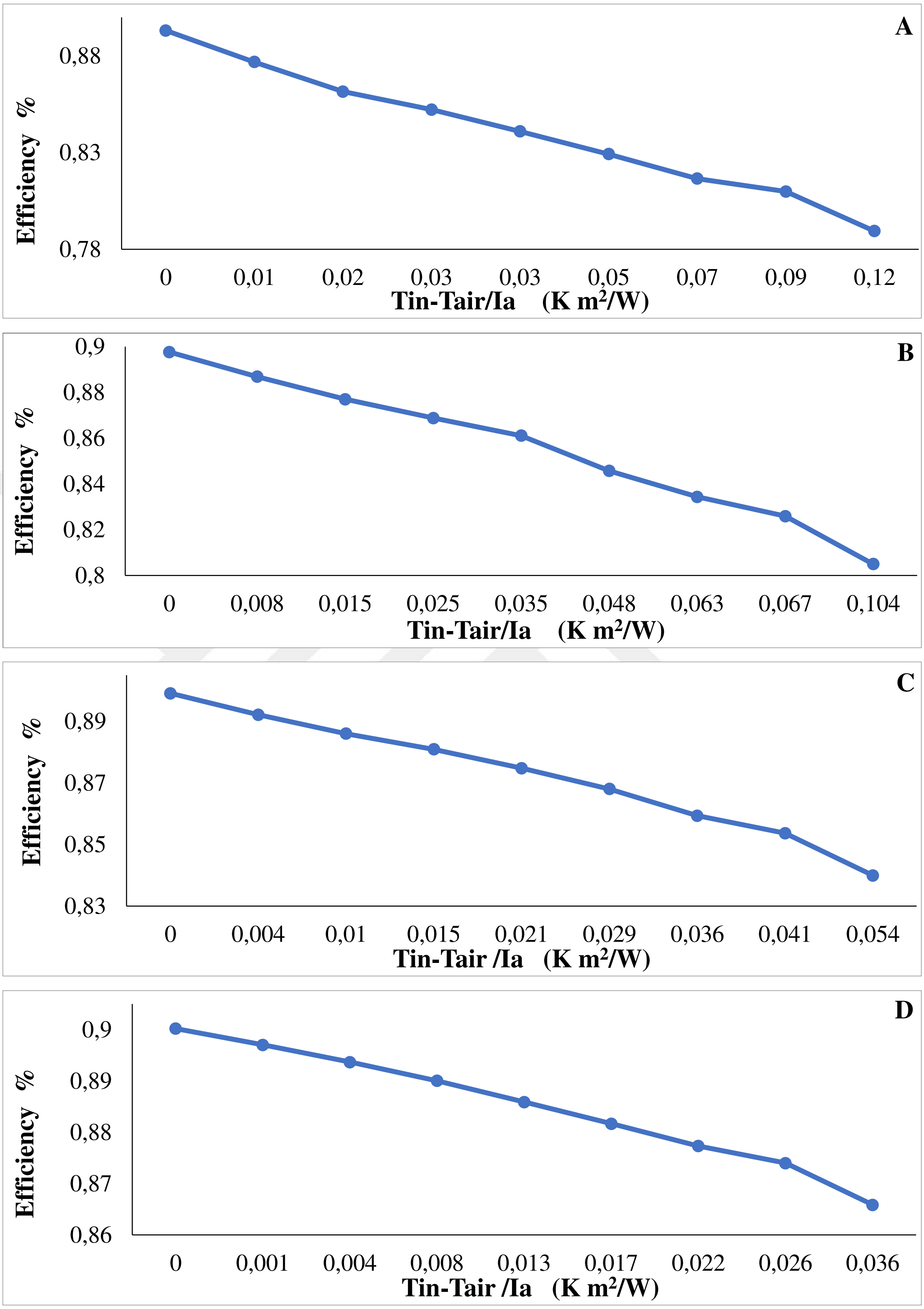

Figure 4.10 Relationship between solar dish collector overall efficiency and operating temperature energy on May 6th (A), May 9th (B), May 12th (C), and May 16th (D)

5. CONCLUSIONS AND RECOMMENDATION

5.1 Conclusions

From the practical results reached in this study, it is concluded that:

- Increasing the efficiency of the solar collector and the gained useful energy by increasing the intensity of solar radiation and the accuracy of placing the receiver in focus,
- The practical, useful energy from the dish solar collector is the highest possible at a mass flow rate of 0.028 kg/s and solar radiation intensity of 940 W/m^2 on day 16th of May so the highest practical, useful energy obtained has reached 1281.26 W,
- The change in the volumetric flow rate of the working fluid (water) has a significant impact on the collector's efficiency,
- Thermal losses increase as the flow rate decreases. That is, the flow rate of 0.0055 kg/s is higher than the flow rate of 0.028 kg/s,
- Thermal losses increase by increasing wind speed,
- The process efficiency is higher at a flow rate of 0.028 kg/s,
- The water temperature entering and exiting the receiver increases with the increase in the intensity of solar radiation,
- The intensity of solar radiation at the time of conducting practical experiments is higher on 16th of May than 6th of May, reaching 940 W/m^2,
- The highest temperature of the water exiting the receiver was on the 6th of May at a flow rate of 0.0055 kg/s, reaching 413 K
- From our study of solar radiation over two months (i.e., April and May), the highest intensity reached in this study was on May 16th, when the intensity reached 940 W/m^2,
- The highest efficiency reached in this study was on the16th of May, at a mass flow rate of 0.028 kg/s,
- The hollow cylindrical receiver is efficient and well-insulated.

5.2 Recommendations

- Increasing the area of the solar concentrator and studying the extent of benefiting from this increase.
- Using reflective materials other than glass to cover the dish and seeing its effectiveness and impact on the efficiency of the solar collector.
- Using different working fluids, such as (water, oil, nanomaterial, Etc.) to detect and study the amount of change they make on the efficiency of the solar collector.
- Using another type of receiver to determine its efficiency and impact on the efficiency of the dish solar collector.
- A numerical analysis can be performed to compare the obtained experimental results with the theoretical results for designing the best dish solar collector.
- Studying the design of receivers of different shapes and detecting their efficiency.

REFERENCES

Abbott, D. 2009. Keeping the energy debate clean: How do we supply the world's energy needs?. Proceedings of the IEEE, 98(1): 42-66.

Aden, B. M. and Meinel, M. P. 1977. Applied solar energy: An introduction. Vol 77. NASA STI/Recon Technical Report A, 33445.

Ahmadi, M. H., Ghazvini, M., Sadeghzadeh, M., Alhuyi Nazari, M., Kumar, R., Naeimi, A., & Ming, T. 2018. Solar power technology for electricity generation: A critical review. Energy Science & Engineering, 6(5): 340-361.

Ahmed, S. M., Al-Amin, M. R., Ahammed, S., Ahmed, F., Saleque, A. M., & Rahman, M. A. 2020. Design, construction and testing of parabolic solar cooker for rural households and refugee camp. Solar Energy, 205: 230-240.

Al Hamadani, A. A. 2019. The Effect of Different Absorber Configurations On The Exergy and The Energy of Parabolic Solar Dish. Wasit Journal of Engineering Sciences, 7(3): 1-13.

Al Hashmi, S. S. A. 2015. Design, Fabrication and Testing of Hybrid Parabolic Dish Concentrator, Stirling Engine & PCM-Storage in Oman. PhD Thesis, University of Leeds, 100 page, Oman.

Alarcón, J. A., Hortúa, J. E., & Lopez, A. 2013. Design and construction of a solar collector parabolic dish for rural zones in Colombia. Tecciencia, 7(14): 14-22.

Aliyu, S. J., Nnodim, C. T., Adebayo, K. R., & Banji, A. A. 2021. Performance Evaluation of Locally Designed and Produced Parabolic Solar Cooker. International Journal of Energy and Environmental Science, 6(4): 96-106.

Alrofiae, A. F. and Kadhem, S. H. 2012. The effects of Sun attraction and solar radiation pressure on Medium Earth orbit Satellites. Journal of Kufa-Physics, 4(2): 20-26.

Alwan, N. T., Shcheklein, S. E., & Ali, O. M. 2020. Experimental investigation of modified solar still integrated with solar collector. Case Studies in Thermal Engineering, 19: 100614.

Amori, K. E., & Sari, R. R. 2018. Thermal performance of parabolıc trough solar collector. The Iraqı Journal for Mechanıcal and Materıals Engıneerıng, 18(3): 389-404.

Augustine, C., Bain, R., Chapman, J., Denholm, P., Drury, E., Hall, D. G., & Young, K. 2012. Renewable Electricity Futures Study. Vol 2, Renewable Electricity Generation and Storage Technologies, United States.

Babuje, A. U., Adamu, J., Tandama, K. U., & Sani, A. 2020. Design, Construction and Testing of a Model Parabolic Trough Solar Collector for Water Heating in Bauchi State. Journal of African Sustainable Development, 20(2): 79-92.

Baharoon, D. A., Rahman, H. A., Omar, W. Z. W., & Fadhl, S. O. 2015. Historical development of concentrating solar power technologies to generate clean electricity efficiently–A review. Renewable and Sustainable Energy Reviews, 41: 996-1027.

Basem, A., Moawed, M., Abbood, M. H., & El-Maghlany, W. M. 2022. The energy and exergy analysis of a combined parabolic solar dish–steam power plant. Renewable Energy Focus, 41: 55-68.

Bissert, P. T., Yantek, D. S., Klein, M. D., & Yan, L. 2016. Analysis of heat loss mechanisms for mobile tent-type refuge alternatives. Transactions of Society for Mining, Metallurgy, and Exploration, 340(1): 70-74.

Bloess, A., Schill, W. P., & Zerrahn, A. 2018. Power-to-heat for renewable energy integration: A review of technologies, modeling approaches, and flexibility potentials. Applied Energy, 212: 1611-1626.

Charran, Z. 2020. Development of an Optical Guide for Parabolic Dish Solar Collectors. PhD Thesis, The University of Western Ontario, 76 page, Canada.

Dafle, V. R. and Shinde, N. N. 2012. Design, development & performance evaluation of concentrating monoaxial Scheffler technology for water heating and low temperature industrial steam application. International Journal of Engineering Research and Applications, 2(6): 1179-1186

Delyannis, E. 2003. Historic background of desalination and renewable energies. Solar energy, 75(5): 357-366.

Duffie, J. A. and Beckman, W. A. 1991. Solar Engineering of Thermal Processes. John Wiley & Sons, 919 page, Indianapolis.

Duffie, J. A. and Beckman, W. A. 1980. Solar Engineering of Thermal Processes. John Wiley & Sons, 782 page, New Yourk.

Duffie, J. A. and Beckman, W. A. 2013. Solar Engineering of Thermal Processes. John Wiley & Sons, 944 page, Indianapolis.

Edenhofer, O., Pichs-Madruga, R., Sokona, Y., Seyboth, K., Kadner, S., Zwickel, T., & Matschoss, P. 2011. Renewable energy sources and climate change mitigation: Special report of the intergovernmental panel on climate change. Cambridge University Press, Cambridge.

European Union Commission. 2012. Directive 2009/28/EC of the European Parliament and of the Council of 23 April 2009 on the promotion of the use of energy from renewable sources and amending and subsequently repealing Directives 2001/77/EC and 2003/30/EC. Official Journal of the European Union, L140/19.

Farret, F. A. and Simões, M. G. 2006. Integration of alternative sources of energy. John Wiley & Sons, 944 page, Hoboken.

Folaranmi, J. 2009. Design, construction and testing of a parabolic solar steam generator. Leonardo Electronic Journal of Practices and Technologies, 14: 115-133.

García-Valladares, O. and Velázquez, N. 2009. Numerical simulation of parabolic trough solar collector: Improvement using counter flow concentric circular heat exchangers. International Journal of Heat and Mass Transfer, 52(3-4): 597-609.

Geyer, M. and Stine, W. B. 2001. Power from the Sun (Powerfromthesun. net). JT Lyle Center.

Goswami, D. Y. 2022. Principles of solar engineering. Taylor & Francis, 656 page, Boca Raton.

Goswami, D. Y., Kreith, F., & Kreider, J. F. 2000. Principles of solar engineering. 2nd edition, Taylor & Francis, 706 page, Boca Raton.

Günther, M., Shahbazfar, R., Fend, T., & Hamdan, M. 2011. Solar dish technology. Advanced CSP teaching materials, 1: 1-63.

Hafez, A. Z., Yousef, A. M., & Harag, N. M. 2018. Solar tracking systems: Technologies and trackers drive types–A review. Renewable and Sustainable Energy Reviews, 91: 754-782.

Hammad, H. J. 2009. Thermal performance of evacuated tube solar heatıng. MSc. Thesis, University of Baghdad, 236 page, Baghdad.

Hassan, A., Quanfang, C., Abbas, S., Lu, W., & Youming, L. 2021. An experimental investigation on thermal and optical analysis of cylindrical and conical cavity copper tube receivers design for solar dish concentrator. Renewable Energy, 179: 1849-1864.

Hijazi, H., Mokhiamar, O., & Elsamni, O. 2016. Mechanical design of a low-cost parabolic solar dish concentrator. Alexandria Engineering Journal, 55(1): 1-11.

Hodges, L. 1982. Resource Letter SE-2: Solar Energy. American Journal of Physics, 50(10): 876-881.

Hosenuzzaman, M., Rahim, N. A., Selvaraj, J., Hasanuzzaman, M., Malek, A. A., & Nahar, A. 2015. Global prospects, progress, policies, and environmental impact of solar photovoltaic power generation. Renewable and Sustainable Energy Reviews, 41: 284-297.

Howell, J. R., Bannerot, R. B., & Vliet, G. C. 1982. Solar-thermal energy systems: analysis and design. Mcgraw Hill Inc., New York.

Iqbal, M. 2012. An introduction to solar radiation. Academic Press, 390 page, Cambridge.

Islam, M. T., Huda, N., Abdullah, A. B., & Saidur, R. 2018. A comprehensive review of state-of-the-art concentrating solar power (CSP) technologies: Current status and research trends. Renewable and Sustainable Energy Reviews, 91: 987-1018.

Jin, X., Xu, G., Zhou, R., Luo, X., & Quan, Y. 2013. A sun tracking system design for a large dish solar concentrator. International Journal of Clean Coal and Energy, 2(2): 16-20.

Kabir, E., Kumar, P., Kumar, S., Adelodun, A. A., & Kim, K. H. 2018. Solar energy: Potential and future prospects. Renewable and Sustainable Energy Reviews, 82: 894-900.

Kadri, Y. and Abdallah, H. H. 2016. Performance evaluation of a stand-alone solar dish Stirling system for power generation suitable for off-grid rural electrification. Energy Conversion and Management, 129: 140-156.

Kalogirou, S. A. 2004. Solar thermal collectors and applications. Progress in energy and combustion science, 30(3): 231-295.

Kasaeian, A., Kouravand, A., Rad, M. A. V., Maniee, S., & Pourfayaz, F. 2021. Cavity receivers in solar dish collectors: A geometric overview. Renewable Energy, 169: 53-79

Khan, J. and Arsalan, M. H. 2016. Solar power technologies for sustainable electricity generation–A review. Renewable and Sustainable Energy Reviews, 55: 414-425.

Kumar, A. and Shukla, S. K. 2015. A review on thermal energy storage unit for solar thermal power plant application. Energy Procedia, 74: 462-469.

Kumar, L., Hasanuzzaman, M., & Rahim, N. A. 2019. Global advancement of solar thermal energy technologies for industrial process heat and its future prospects: A review. Energy Conversion and Management, 195: 885-908.

Liu, M., Tay, N. S., Bell, S., Belusko, M., Jacob, R., Will, G., & Bruno, F. 2016. Review on concentrating solar power plants and new developments in high temperature thermal energy storage technologies. Renewable and Sustainable Energy Reviews, 53: 1411-1432.

Loni, R., Najafi, G., Mamat, R., Ghazali, M. F., & Sidik, N. A. C. 2022. Nusselt Number Prediction for Oil and Water in Solar Tubular Cavity Receivers. Journal of Advanced Research in Fluid Mechanics and Thermal Sciences, 97(2): 157-174.

Luceño, J. A., de la Fuente, E., & Martin, M. 2021. Optimal Design of Solar Receivers in CSP Plants: Effects of Facility Location. Industrial & Engineering Chemistry Research, 60(19): 7218-7231.

Madadi, V., Tavakoli, T., & Rahimi, A. 2014. First and second thermodynamic law analyses applied to a solar dish collector. Journal of Non-Equilibrium Thermodynamics, 39(4): 183-197.

Mahmood, Y. H. and Al-Salih, R. Y. 2018. Experimental study of two different types of solar dish characteristics and its efficiency based on Tikrit, Iraq weather conditions. In Journal of Physics: Conference Series, 1032(1): 012006.

Mahmood, Y. H., Munef, R. A., & Bazzaz, A. A. 2015. Modulating a Solar Parabolic Dish to Produce Boiled Water. Journal of Environmental Science and Engineering, A4: 225-232.

Majeed, M. H., Alwan, N. T., Shcheklein, S. E., & Matveev, A. V. 2021. Electromechanical solar tracker system for a parabolic dish with CPU water heater. Materials Today: Proceedings, 42: 2346-2352.

Mancini, R. 2015. Volumetric Solar Receiver for a Parabolic Dish and Micro-Gas Turbine system: Design, modelling and validation using Multi-Objective Optimization. MSc thesis, 113 page, KTH Royal Institute of Technology, Stockholm.

Mohamed, E. A. and Eltahir, M. 2013. Design and testing of a solar parabolic concentrating collector. Renewable Energy and Power Quality Journal, 1(11): 72-76.

Mohamed, F. M., Jassim, A. S., Mahmood, Y. H., & Ahmed, M. A. 2012. Design and study of portable solar dish concentrator. International Journal of Recent Research and Review, 3: 52-59.

Mohammed, I. L. 2012. Design and development of a parabolic dish solar water heater. International Journal of Engineering Research and Applications, 2(1): 822-830.

Mohammed, I. L. 2013. Design and development of a parabolic dish solar thermal cooker. International Journal of Engineering Research and Applications, 3(4): 1179-1186.

Mohammed, I. L., & Bartholomew, P. N. 2012. Development Of Control Cırcuıt For Parabolıc Dısh Solar Water Heater. International Journal of Advances in Engineering & Technology, 3(2): 16-25.

Naveenkumar, R., Ravichandran, M., Mohanavel, V., Karthick, A., Aswin, L. S. R. L., Priyanka, S. S. H., & Kumar, S. P. 2022. Review on phase change materials for solar energy storage applications. Environmental Science and Pollution Research, 29: 9491-9532.

Newton, C. C. 2007. A Concentrated Solar Thermal Energy System. MSc thesis, 179 page, Florida State University, Florida.

O'Gallagher, J. J. 2008. Nonimaging optics in solar energy. Part of the book series: Synthesis Lectures on Energy and the Environment: Technology, Science, and Society, Morgan and Claypool Publishers, 120 page, California .

Omara, Z. M. and Eltawil, M. A. 2013. Hybrid of solar dish concentrator, new boiler and simple solar collector for brackish water desalination. Desalination, 326: 62-68.

Owaıd, A. I., Tarıq, M., Mustafa, F. I., Alwan, K., & Yassın, T. 2014. Effect of Successive Cloudy Days on Operating the Solar Space Heating System using Evacuated Tubes Solar Collector in Baghdad-Iraq Climate. International Journal of Scientific Engineering and Tcehnology Research, 3(4): 544-549.

Pandey, A. K., Tyagi, V. V., Jeyraj, A., Selvaraj, L., Rahim, N. A., & Tyagi, S. K. 2016. Recent advances in solar photovoltaic systems for emerging trends and advanced applications. Renewable and Sustainable Energy Reviews, 53: 859-884

Patil, P. N., Khandekar, M. A., & Patil, S. N. 2016. Automatic dual-axis solar tracking system for parabolic dish. In 2016 2nd International Conference on Advances in Electrical, Electronics, Information, Communication and Bio-Informatics, pp. 699-703, Chennai.

Pawar, J. B. And Tungikar, V. B. 2022. An experimental examination of a helically coiled conical cavity receiver with Scheffler dish concentrator in terms of energy and exergy performance. Sustainable Energy Technologies and Assessments, 52: 102221

Rabl, A. 1985. Active solar collectors and their applications. Oxford University Press, 526 page, Oxford.

Răboacă, M. S., Badea, G., Enache, A., Filote, C., Răsoi, G., Rata, M., & Felseghi, R. A. 2019. Concentrating solar power technologies. Energies, 12(6): 1048.

Rafeeu, Y. and Ab Kadir, M. Z. A. 2012. Thermal performance of parabolic concentrators under Malaysian environment: A case study. Renewable and Sustainable Energy Reviews, 16(6): 3826-3835.

Raguram, A. and Lingeswaran, K. 2014. Design of Stirling Engine and Solar Collectors to Run an Automobile Alternator. Middle-East Journal of Scientific Research, 20(7): 815-818.

Rajamohan, G., Kumar, P., Anwar, M., & Mohanraj, T. 2017. Analysis of solar water heater with parabolic dish concentrator and conical absorber. In IOP conference series: materials science and engineering, 206 (1): 012030.

Rapp, A., Agnihotri, R., & Forbes, L. P. 2008. The sales force technology–performance chain: The role of adaptive selling and effort. Journal of Personal Selling & Sales Management, 28(4): 335-350.

REN21. 2008. Renewables 2007 Global Status Report. REN21 Secretariat, Paris.

Romero, M. and Steinfeld, A. 2012. Concentrating solar thermal power and thermochemical fuels. Energy & Environmental Science, 5(11): 9234-9245.

Sagade, A. A. 2015. Experimental investigation of effect of variation of mass flow rate on performance of parabolic dish water heater with non-coated receiver. International Journal of Sustainable Energy, 34(10): 645-656.

Sagade, A. A., Mawire, A., Belgasim, B., Tawfik, M. A., & Sagade, N. A. 2021. Experimental performance evaluation of a parabolic dish solar geyser using a generalized approach for decentralized applications. Sustainable Energy Technologies and Assessments, 47: 101454

Sakhare, V. and Kapatkar, V. N. 2014. Experimental analysis of parabolic solar dish with copper helical coil receiver. International Journal of Innovative Research in Advanced Engineering, 1(8): 199-204.

Sharma, A. 2011. A comprehensive study of solar power in India and World. Renewable and Sustainable Energy Reviews, 15(4): 1767-1776.

Spelling, J. 2011. Steam Turbine Optimisation for Solar Thermal Power Plant Operation. PhD thesis, KTH Royal Institute of Technology,100 page, Stockholm.

Starakis, I. and Halkia, K. 2010. Why is it hotter in Summer than in Winter? K-5 Students and Pre-service Elementary Teachers' Conceptions of Seasonal Change. In XIV IOSTE Symposium: 13-18, Slovenia.

Stattman, S. L., Gupta, A., Partzsch, L., & Oosterveer, P. 2018. Toward sustainable biofuels in the European Union? Lessons from a decade of hybrid biofuel governance. Sustainability, 10(11): 4111.

Strantzali, E. and Aravossis, K. 2016. Decision making in renewable energy investments: A review. Renewable and sustainable energy reviews, 55: 885-898

Sulaiman, F., Abdullah, N., & Singh, B. S. M. 2012. A simulated design and analysis of a solar thermal parabolic trough concentrator. International Journal of Environmental and Ecological Engineering, 6(12): 739-743.

Swanepoel, J. K. 2019. Helically coiled cavity receiver for a micro-scale direct generation steam Rankine cycle using a novel solar dish design. PhD thesis, University of Pretoria, 75 page, Pretoria.

Swanepoel, J. K., le Roux, W. G., Lexmond, A. S., & Meyer, J. P. 2021. Helically coiled solar cavity receiver for micro-scale direct steam generation. Applied Thermal Engineering, 185: 116427

Tadros, M. T. Y., Mustafa, M. A. M., & Abdel-Wahab, M. 2014. Estimation of the global horizontal solar radiation in Iraq. International Journal of Emerging Technology and Advanced Engineering, 4(8): 587-605.

Tauseef, S. M., Abbasi, T., & Abbasi, S. A. 2013. Energy recovery from wastewaters with high-rate anaerobic digesters. Renewable and Sustainable Energy Reviews, 19: 704-741

Teles, M. R., Carvalho, R., & Ismail, K. A. 2017. Optical analysis of low concentration evacuated tube solar collector. Advances in Energy Research, 5(3): 227-237.

Thakkar, V., Doshi, A., & Rana, A. 2015. Performance analysis methodology for parabolic dish solar concentrators for process heating using thermic fluid. Journal of Mechanical and Civil Engineering, 12(1): 101-114.

Tian, Y. and Zhao, C. Y. 2013. A review of solar collectors and thermal energy storage in solar thermal applications. Applied energy, 104: 538-553.

Wang, J., Zhang, J., Cui, Y., & Bi, X. 2016. Design and implementation of PLC-based automatic sun tracking system for parabolic trough solar concentrator. In MATEC Web of Conferences, 77: 06006.

Wu, S. Y., Xiao, L., Cao, Y., & Li, Y. R. 2010. A parabolic dish/AMTEC solar thermal power system and its performance evaluation. Applied Energy, 87(2): 452-462.

Zedan, M. H., Khalaf, H. J., & Shaker, A. M. 2017. Optimum Design of Parabolic Solar Collector with Exergy Analysis. Tikrit Journal of Engineering Sciences, 24(4): 49-57.

Zhu, Z., Zhang, D., Mischke, P., & Zhang, X. 2015. Electricity generation costs of concentrated solar power technologies in China based on operational plants. Energy, 89: 65-74.

APPENDICES

APPENDIX 1. Photos of the system and test setup

APPENDIX 2. Calculating the engineering characteristics and the heat transfer processes

APPENDIX 1. Photos of the system and test setup

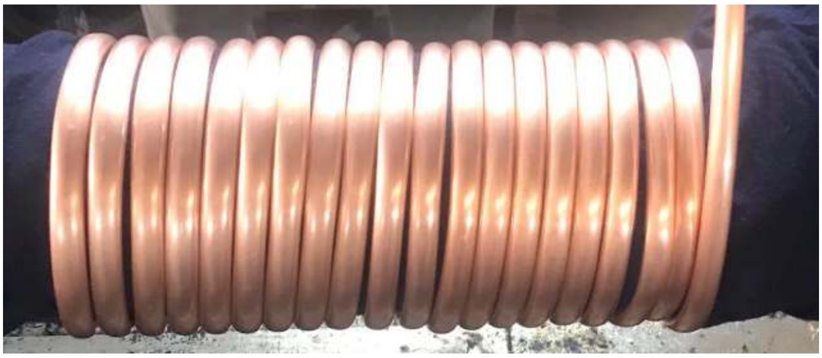





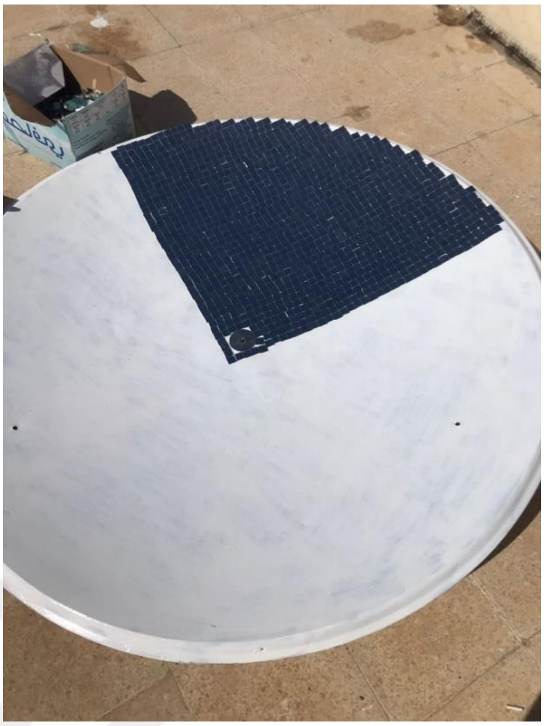

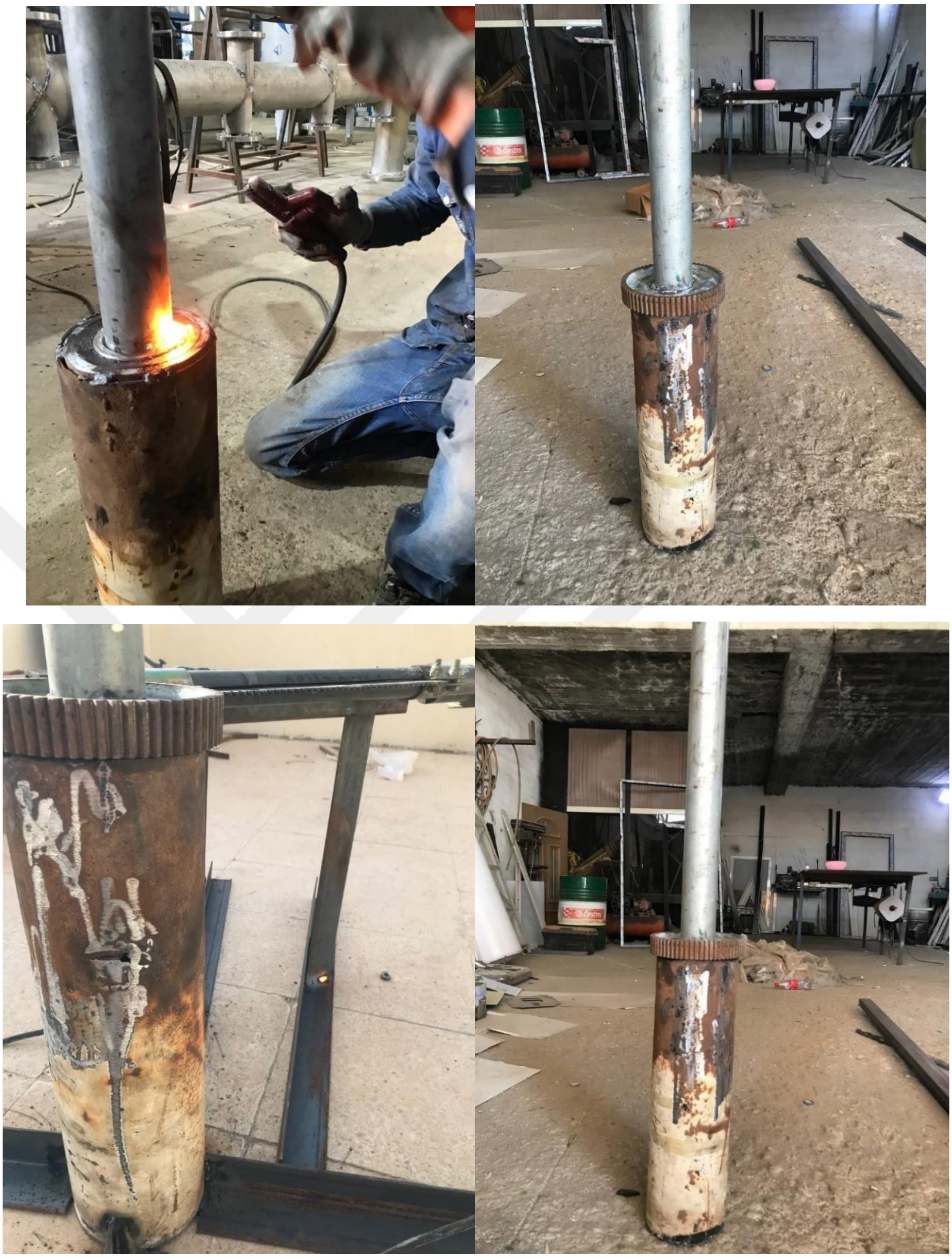






APPENDIX 2. Calculating the engineering characteristics and the heat transfer processes

Calculating the engineering characteristics of the stratified solar collector using the Excel program through the following equations:

$$CR = \frac{A_a}{A_r}$$

$$CR = \frac{1.5386}{0.0181} = 84.83$$

Where:

- CR: Concentration ratio
- A_a: Collector aperture area

The focal length is given by the following equation:

$$f = \frac{d^2}{16 .h}$$

$$f = \frac{(1.4)^2}{16 \text{ x } 0.14} = 0.875 \text{ m}$$

Where:

- h: Depth of concentrators
- d: Collector orifice diameter
- f: Represents the focal length
- Tan φ rim Rim angle

$$\text{Tan } \varphi \text{ rim} = \frac{1}{\frac{d}{8.h} - \frac{2.h}{d}}$$

$$\text{Tan } \varphi \text{ rim} = \frac{1}{\frac{1.4}{8 \text{ x } 0.14} - \frac{2 \text{ x } 0.14}{1.4}} = 43.6$$

The surface area of the solar concentrator

$$\text{A Concentrator surface area} = \frac{2\ \pi}{3\ P}\ [\sqrt{(\frac{D^2}{4} + P^2)^3} - P^3]$$

$$\text{where } P = \frac{D^2}{8\text{ H}} = \frac{(1.4)^2}{8 \text{ x } 0.14} = 1.75 \text{ m}$$

$$\text{A Concentrator surface area} = \frac{2 \text{ x } 3.14}{3 \text{ x } 1.75} \left[\sqrt{(\frac{(1.4)^2}{4} + (1.75)^2)^3} - (1.75)^3\right]$$

$$= 1.599 \text{ m}^2$$

$$\text{A Concentrator Aperture area} = \pi\ (\frac{D}{2})^2 = 3.14 \text{ x } (\frac{1.4}{2})^2 = 1.5386 \text{ m}^2$$

Dimensions of Receiver

$$A_{base} = \pi\ (\frac{D}{2})^2 = 3.14\ (\frac{0.152}{2})^2 = 0.0181\ m^2$$

$$A_{sides} = d\ \pi\ h = 0.152\ x\ 3.14\ x\ 0.23 = 0.109\ m^2$$

$$A_{receiver} = A_{base} + A_{sides} = 0.0181 + 0.109 = 0.127\ m^2$$

Calculating the heat transfer processes of the stratified solar collector using the Excel program through the following equations:

h_r: Radiation heat transfer coefficient:

$$h_r = 4\ \sigma\ \varepsilon\ T_{mean}^3$$

$$h_r(1) = 4 \text{ x } 5.67 \text{ x } 10^{-8} \text{ x } 0.5 \text{ x } (304)^3 = 3.186 \text{ W/m}^2 \text{ K}$$

$$h_r(2) = 4 \text{ x } 5.67 \text{ x } 10^{-8} \text{ x } 0.5 \text{ x } (307)^3 = 3.28 \text{ W/m}^2 \text{ K}$$

σ: Stefan-Boltzmann constant = 5.67×10^{-8} W/m^2 K^4

ε: Reflective surface emission

T_{mean}: The temperature of the atmosphere surrounding the work area (K)

The appropriate equation for calculating Nusselt Nipper depends on Reynolds Nipper for air Rea according to the following:

$Nu = 0.4 + 0.54\ Re^{0.52}$ for $0.1 < Re < 1{,}000$

$Nu = 0.3\ Re^{0.6}$ for $1{,}000 \le Re < 50{,}000$

Re The Reynolds Nipper of air can be found in the following equation:

$$Re = \frac{V\ D_{outer}}{v}$$

$$Re\ (1) = \frac{(0.2 \text{ x } 0.152)}{(5.15 \text{ x } 10^{-5})}$$

Re (1) = 590.291

$$\text{Re }(2) = \frac{(0.35 \text{ x } 0.152)}{(5.15 \text{ x } 10^{-5})}$$

Re (2) = 1033.01

Where:

- V is the speed of air
- v is the air viscosity
- D_{outer} is the outside diameter of the receiver

Nu: Nusselt Nipper can be found from the following equation:

$$\text{Nu} = 0.4 + 0.54\ \text{Re}^{0.52}$$

$$\text{Nu }(1) = 0.4 + 0.54 \text{ x } (590.291)^{0.52}$$

$$\text{Nu} = 15.31$$

$$\text{Nu }(2) = 0.3\text{x } (1033.01)^{0.6}$$

$$\text{Nu }(2) = 19.30$$

h_w: the convection coefficient and is given by the following equation:

$$h_w = \frac{k_{air}}{D_{outer}} \ .\ Nu$$

$$h_w(1) = \frac{0.0456}{0.152}\ x\ 15.31 = 4.59\ \text{W/m}^2\ \text{K}$$

$$h_w(2) = \frac{0.0456}{0.152}\ x\ 19.30 = 5.79\ \text{W/m}^2\ \text{K}$$

k_{air} : Thermal conductivity of air 0.0456 W/m K

UL is the Overall heat loss coefficient

$$U_L = [\frac{1}{h_w - h_r}]^{-1}$$

$U_L(1) = [\frac{1}{4.59-3.186}]^{-1} = 7.777$ W/m² K

$U_L(2) = [\frac{1}{4.79-3.28}]^{-1} = 9.07$ W/m² K

Tr: The average temperature of the receiver is given by the following equation

$$Tr = \frac{T_{in} + T_{out}}{2}$$

$Tr = \frac{304+318}{2} = 311$ K

The following equation gives the optical energy absorbed by the receiver:

$$Q_{opt} = A_a \ \rho_{s\_m} \ \tau_g \ \alpha_r \ S \ I_b$$

$Q_{opt}(1) = 1.5386$ x 1 x 1 x 0.95 x 480 x 0.95 $= 666.52$ W

$Q_{opt}(2) = 1.5386$ x 0.95 x 1 x 0.95 x 480 x 0.95 $= 1166.41$ W

The following equation gives the heat losses lost from the receiver:

$$Q_{loss} = A_r \ U_L \ (T_r - T_a)$$

$Q_{loss}(1) = 0.1279$x 7.777 x $(311 - 304) = 6.964$ W

$$Q_{loss}(2) = 0.1279x\ 9.07\ x\ (363 - 307) = 64.981\ W$$

The following equation gives the useful energy absorbed by the water:

$$Q_{out} = Q_{opt} - Q_{loss}$$

$$Q_{out}\ (1) = 666.52 - 6.964 = 659.56\ W$$

$$Q_{out}\ (2) = 1166.41 - 64.981 = 1101.43\ W$$

The following equation gives the total efficiency of the collector:

$$\eta_{collector} = \frac{Q_{out}}{Q_s} = \frac{Q_{out}}{I_b\ A_a}$$

$$\eta_{collector}(1) = \frac{659.56}{480\ x\ 1.5386} = 0.89$$

$$\eta_{collector}(1) = \frac{1101.43}{840\ x\ 1.5386} = 0.85$$

CURRICULUM VITAE

Personal Information

Name and Surname : Wisam Mohammed Fayyadh FAYYADH

Education

MSc	Çankırı Karatekin University Graduate School of Natural and Applied Sciences Department of Physics	2021-2023
Undergraduate	University of Tikrit College of Science Department of Physics	2007-2011

Work Experience

Year	**Institution**	**Position**
2000-2012	Iraqi Ministry of Electricity, General Company for Electricity Production/North	Technician & Supervisor Boilers and Rotatory Pumps
2012-2014	Iraqi Ministry of Electricity, General Company for Electricity Production/North	Head of Unit Training & Development
2015-Present	Iraqi Ministry of Electricity, General Company for Electricity Production/North	Head of Unit Engineering Examinations

Academic Activities

1. Participated in several courses in the field of education and skills development, Boilers, fine instruments, occupational safety, computers.
2. Participated in many courses related to non-destructive tests,